

EXPERIMENTAL STUDIES OF SIMULATED GOUGE AND THEIR APPLICATION
TO STUDIES OF NATURAL FAULT ZONES

by

John M. Logan, M. Friedman, N. Higgs, C. Dengo, and T. Shimamoto*
Center for Tectonophysics
Texas A&M University
College Station, Texas 77843

ABSTRACT

Laboratory studies of simulated gouge materials have yielded considerable observational information of the deformed material. The studies reported here emphasize (1) development of simulated fault zones, (2) changes in fault zone fabric with increasing temperature, (3) fracture patterns developed in simulated gouges, and (4) the value of these experimental results to field investigations. The results show that when fracture and cataclasis are the principle mechanisms of behavior of the simulated gouge, the deformation becomes heterogeneous within a few millimeters of initial displacement. Although R_1 fractures are well developed, most of the displacement is accommodated in a very narrow zone at or close to the gouge-rock interface. With increasing temperature, simulated gouges of calcite undergo a transition from stick-slip to stable sliding at about 400°C, and 200 MPa confining pressure. This transition is accompanied by a change from cataclastic deformation of the gouge to ductile flow by intracrystalline mechanisms. The displacement zone within the gouge widens to encompass the total gouge zone. At 600°C recrystallization resulting in small crystals occurs during steady state behavior. At about 900°C, the stress-strain curve shows work softening and the recrystallized grain size has increased by a factor of 30. A well developed fracture array is developed within the cataclastic gouge, with R_1 and R_2 Riedel shears and P fractures best displayed. Studies of natural fault zones, particularly the Motagua fault, show a marked correlation of the fractures with the experimental studies. Here R_1 , P and Y fractures are well defined. To date there is no definitive deformational features indicative of stick-slip, although ductile flow does appear to be uniquely associated with stable sliding. Cataclastic behavior is found to occur with either stick-slip or stable sliding.

INTRODUCTION

The problem of earthquake prediction necessitates an understanding of earthquake source mechanisms which is in turn dependent upon our understanding of fault zone properties. The mechanical behavior of the country rock-fault gouge system, as well as the physical properties of permeability, fluid saturation, elastic moduli, thermal conductivity, etc., must be known if intelligent predictions of earthquakes are to be made. Additionally, this information is necessary for an understanding

*Current address: Institute of Geology and Mineralogy, Hiroshima University, Higashi-senda cho, Hiroshima, 730 Japan.

of problems such as, thrust-plate movement, rifting, and flexural slip folding, all of which involve movement of rock along planes or zones. Embarrassingly, little is known about the requisite mechanical and physical properties. This becomes very evident when one inquires about the geometry of fault surfaces of geologists, let alone the more complex problem of composition, fabric and sites of displacement, or estimates of mechanical behavior or other physical properties such as fracture geometry and distribution, permeability, or fluid saturation. Our lack of knowledge may in part be dependent upon a variety of factors. (1) There are frequently no exposures of sufficient vertical and lateral extent to provide useful information. (2) There is considerable uncertainty as to what extent studies carried out on surface exposures, however exhaustive and informative, apply to material beneath the Earth's surface. (3) The multitude of features to be studied in the field, and the difficulty of finding comparable exposures, precludes rapid assessment of parameters. (4) It is frequently difficult, if not impossible, to recognize the important from the minor factors influencing deformation or to develop a temporal sequence of the development of fault zone features.

In an attempt to provide another tool for investigating these problems, laboratory investigations have been undertaken to look at simulated gouge materials (Engelder et al., 1975; Logan, 1975; Logan and Shimamoto, 1976; Summers and Byerlee, 1977; Shimamoto, 1977; Byerlee et al., 1978). This approach, however simplistic, allows the isolation and evaluation of given parameters, the assessment of the development of the simulated zone through time and with limited displacement, the measurement of changes in other physical properties such as permeability and porosity, and an evaluation of the fabric of the simulated fault zone. In the present paper we would like to summarize the conclusions of laboratory investigations by considering the following areas: (1) development of simulated fault zones, (2) changes in fault zone fabric with increasing temperature, (3) fracture patterns developed in laboratory investigations, and (4) the value of experimental results to field investigations. These topics will be treated in this order, but it is informative to briefly review the experimental procedure utilized in these studies.

Most experiments have been conducted on right circular cylinders containing a sawcut at 35° to the cylinder axis. Simulated gouge is created by disaggregating and then grinding rocks of the desired composition. The resulting material is sieved to give a known particular size distribution and then spread along the sawcut. The simulated gouge layers range from 0.5 to 5 mm thick. The specimen is then jacketed and deformed in triaxial compression. Confining pressures to 600 MPa (Byerlee and Summers, 1973, 1976), temperatures to 900°C (Higgs and Logan, 1977) and displacement rates of 10^{-3} to 10^{-7} cm/sec have been employed. A variety of materials have been used ranging from quartz and granite through halite and montmorillonite (Engelder et al., 1975; Byerlee et al., 1978; Shimamoto, 1977), and mixtures of these components (Shimamoto, 1977). Stable sliding, stick-slip and the transition from one to the other has been observed (Logan, 1975; Higgs and Logan, 1977; Shimamoto, 1977).

DEVELOPMENT OF SIMULATED FAULT ZONES

Compaction of Simulated Gouge

Evidence accumulated to date supports the hypothesis that although the simulated gouge starts as an unconsolidated aggregate of high porosity, **it** is transformed after a few millimeters of displacement to consolidated, "lithified" material of reduced porosity. The grain size reduction accompanying a few millimeters of displacement is well documented (Figure 1), and apparently is accomplished within three millimeters of displacement in these experiments. This decrease in grain size is also accompanied by a decrease in porosity (Table 1), and presumably a decrease in permeability, although the latter has not been documented. **It** has been shown that the application of confining pressure alone is not sufficient to produce the grain size reduction but that some shear displacement must also take place (Logan and Shimamoto, 1976). Accompanying the grain size and porosity reduction is an apparent consolidation, compaction and "lithification" of the simulated gouge, **so** that when the specimen is opened after an experiment, the simulated gouge is now a coherent layer of rock material.

During the grain size reduction the displacement within the simulated gouge zone is **more** or less homogeneously distributed within the zone, but as the grain size is reduced, the energy to continue this reduction is increased to such a level that the displacement no longer occurs homogeneously, but now appears to be concentrated along distinct planar zones within the gouge zone (Figure 2) and at the interface with the country rock. This concept of heterogeneous distribution of displacements differs from the assumptions made in some theoretical models (e.g., Stuart, 1974). The question remains as to where most of the displacement takes place. That is, does **it** occur at the rock-gouge interface, along the inclined shear zones or distributed between both sites.

Deformation near the Country Rock-Gouge Interface

In some of their shearing experiments of quartz powder, Griggs and others (1960, p. 50) recognized that the samples had not been sheared internally and slip had taken place between the steel piston and the sample. More recently, Engelder (1973, 1974) and Engelder et al. (1975), from a study of deformed quartz gouge during the frictional sliding of Tennessee sandstone, pointed out that at confining pressures above 40 MPa, **deformation** becomes concentrated along the interface between the country rock and gouge during the sliding. Direct supporting evidence for this is the extreme grain-size reduction and the development of indurated gouge at the interface (see Engelder et al., 1975, p. 78). The grain size of the deformed quartz is distributed nearly uniformly throughout the major portion of the gouge (except at discrete planar structures developed within the gouge; see next subsection). This implies that a shift in the mode of deformation from pervasive cataclastic flow of gouge to concentrated deformation along the country

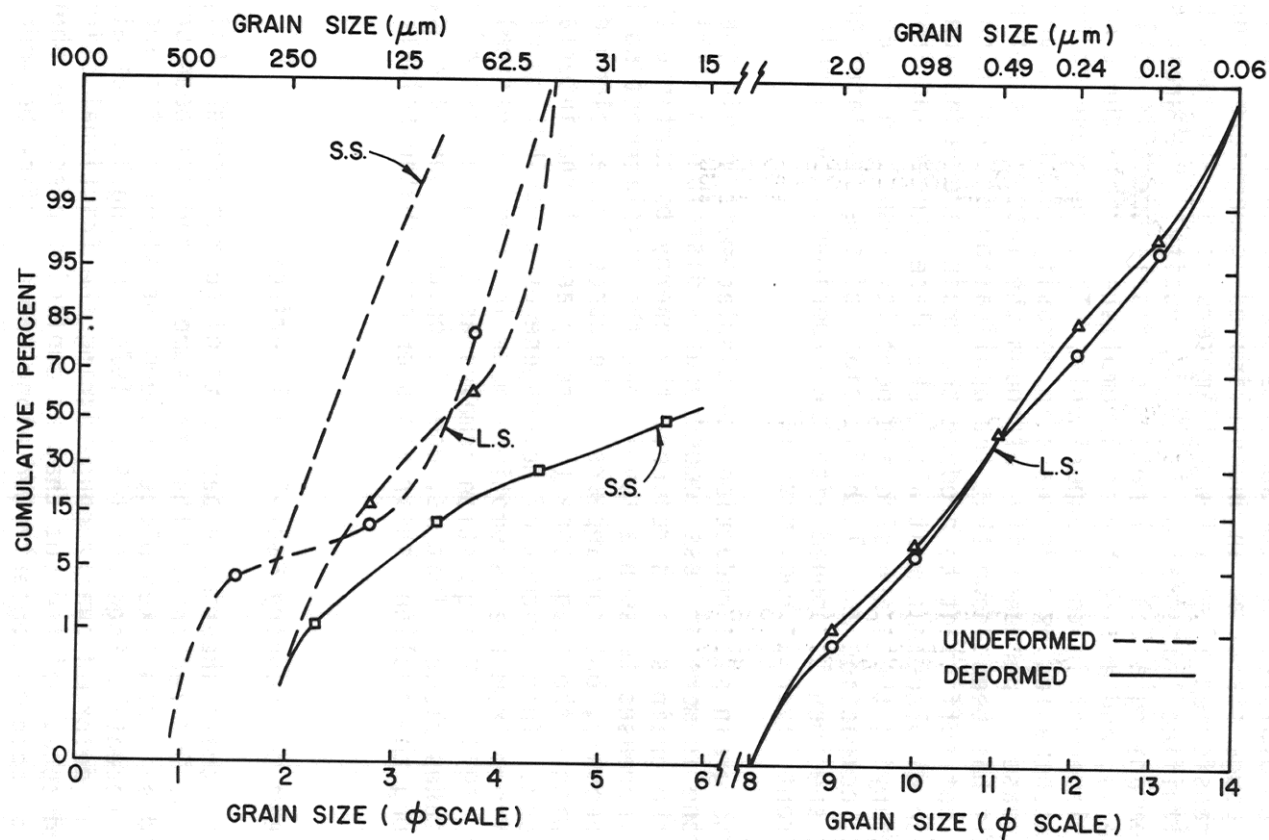
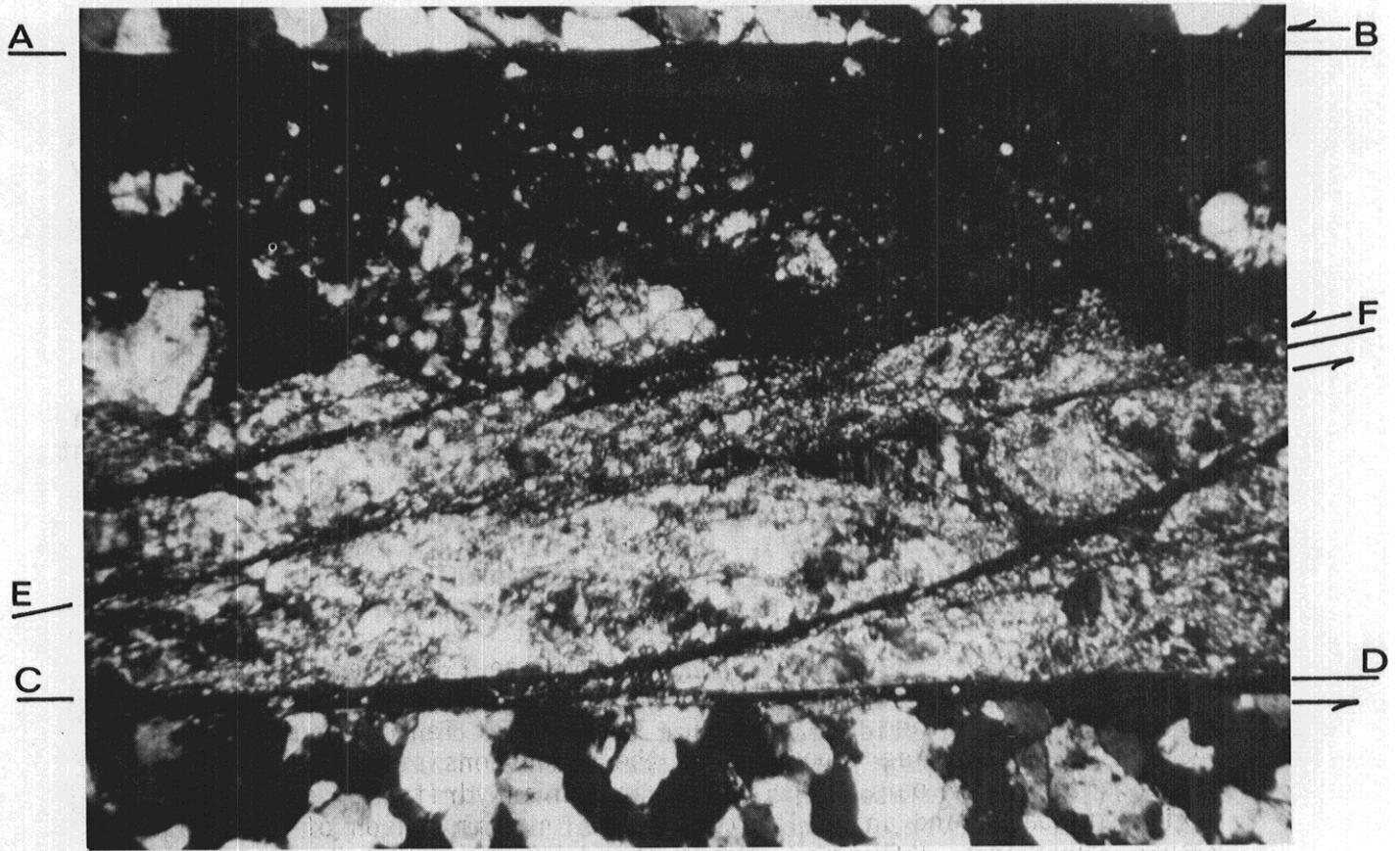


Figure 1. Cumulative frequency curves for simulated gouge, 2 mm thick distributed along a 35° saw-cut surface of Tennessee sandstone. The specimens were deformed at 50 MPa, 25°C , and a constant rate of displacement of 10^{-3} cm/sec. The dashed lines represent undeformed material of quartz (S.S.) and calcite (L.S.), and the solid lines show the size distribution after 1.2 mm displacement.

Table 1. Experimental Gouge-Porosity Measurements

Type of Gouge	Density (g/cm ³)	Porosity Before (%)	Porosity After (%)	Confining Pressure (MPa)	Displacement (cm)
Quartz	1.69	36.2	9	100	1.4
Garnet	2.25	42.4	11	100	1.3
Pyrite	2.83	43.3	5	100	1.3
Orthoclase	1.28	50.5	6	100	1.3
Apatite	1.72	45.4	4	50	1.4
Dolomite	1.35	52.5	3	50	1.3
Fluorite	1.81	42.9	3	70	1.4
Anhydrite	1.66	43.7	2	50	1.3
Calcite	1.51	44.3	2	75	1.4
Galena	3.52	53.3	1	100	1.5
Barite	2.44	45.6	1	110	1.5
Halite	1.35	37.4	<1	100	1.5

Figure 2. Photomicrographs of quartz-anhydrite two-layer gouge deformed dry at a pressure of 100 MPa; crossed polarized light. Upper photo, gouge zone is confined by the precut surfaces of Tennessee sandstone (AB and CD). Upper dark portion of the gouge consists mainly of quartz. Although the lower part of gouge is rich in anhydrite, a considerable mixing of quartz and anhydrite took place in this region of the gouge. Planar structures, R₁ Riedel shears, are well developed in the gouge at an angle of 10-20° to the sliding surface (e.g., EF in the photograph). Scale is 0.6 mm. Lower photo, a close-up of the central portion of photograph (a). Observe that a fractured quartz grain with undulatory extinction has displaced along the planar structure EF. Scale is 0.2 mm.



a



b

rock-gouge interface is considerably abrupt. Using photomicrographs of deformed quartz gouge taken with a transmission electron microscopic (TEM), Engelder (1973, p. 100) determined that the average grain size of quartz near the rock-gouge interface is about $0.2 \mu\text{m}$. This is roughly two orders of magnitude smaller than the average grain size in the major portion of the gouge (about $30 \mu\text{m}$; Engelder, 1974, Fig. 11).

Additional evidence to support the contention that the major displacement occurs at the simulated gouge-rock interface as derived from observations of the deformed specimens (Figure 3). In the simulated gouge of calcite, pyrite impurities are present. Those at the interface with the country rock were deformed and smeared out. The measured length of these streaks is very close to that measured for the total displacement of the gouge zone. Similar correlations have been found by introducing theomodye at the interface, which also becomes smeared out during the deformation (Shimamoto, 1977). Chatter marks on the rock surface at the interface and sheared grains all support the conclusion that most of the displacement occurs at this site (Logan and Shimamoto, 1976).

All of these observations indicate that the deformation of gouge no doubt becomes concentrated near the country rock-gouge interface during the frictional sliding, and that a relative displacement of the country rock and gouge does take place at their boundary. Engelder and others (1975) correlated this shift of deformation with the onset of stick-slip. However, the concentration of deformation itself is not always associated with stick-slip. For instance, only stable sliding occurs during the deformation of quartz and dolomite gouges, although clear evidence exists for displacement at the interfaces (Shimamoto, 1977). Although the intense deformation of gouge near the rock-gouge interface may have significant implications for the stick-slip mechanisms, the shift in the mode of gouge deformation cannot be directly correlated with the stable sliding to stick-slip transition.

The next question is whether the displacement occurs along both rock-gouge interfaces or along one of them. The problem has been examined in terms of the presence of slickenside surfaces and the pattern of smear marks on deformed gouges. In most cases examined, the relative displacement occurs along only one of the rock-gouge interfaces, although there is no a priori reason why this has to be so. Occasionally, however, the displacement takes place on both interfaces. And in some cases, the relative displacement occurs along one interface in some regions of gouge, whereas it takes place along the other interface in other regions. This of course, is expected when one of the interfaces is more tightly locked than the other interface in a certain domain of the gouge.

Deformation Along Distinct Planar Zones within Gouge

Concentration of deformation along distinct planar structures within the gouge has been pointed out by Engelder (1973, 1974) for quartz gouge deformed with Tennessee sandstone, by Logan and Shimamoto (1976) for dolomite gouge deformed with Tennessee sandstone, and by Byerlee and

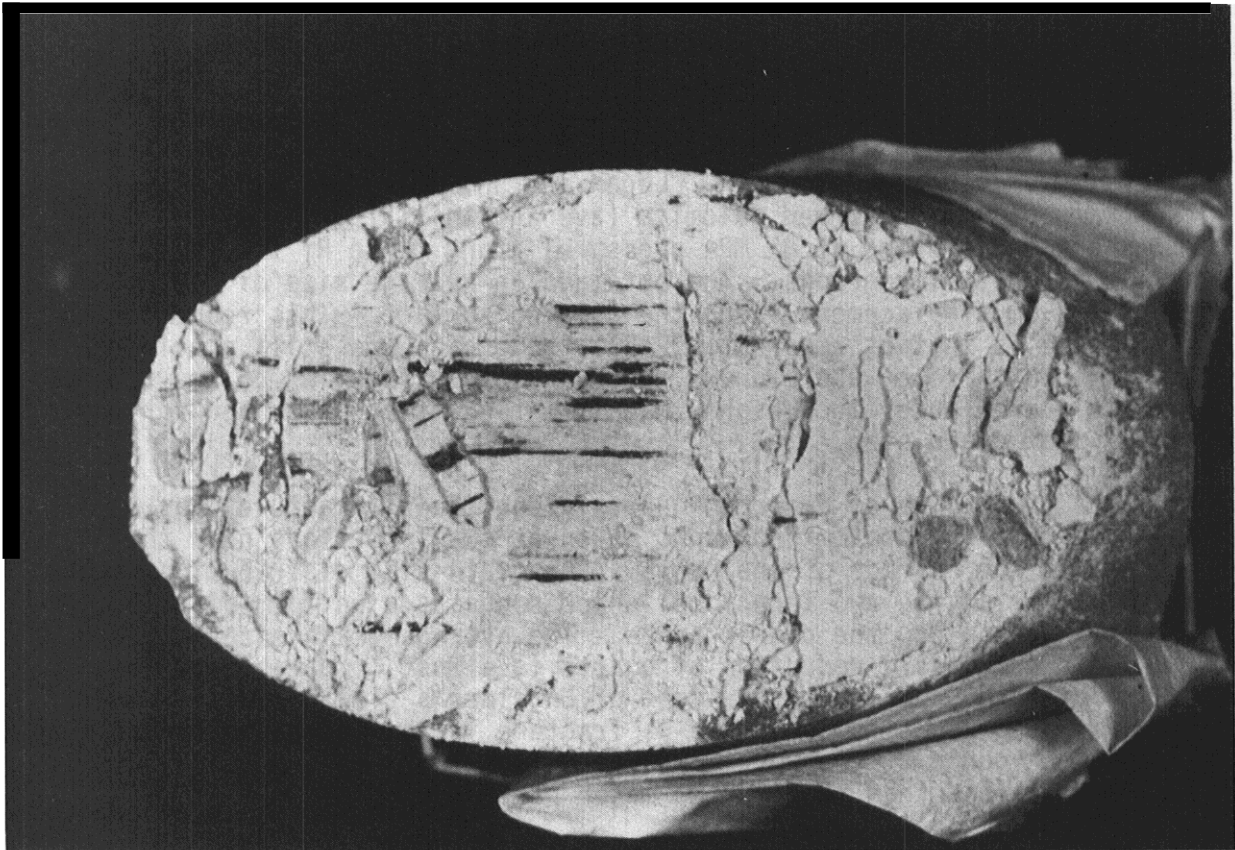


Figure 3. Specimen with simulated gouge of calcite scraped off part of the sawcut exposing the streaks of deformed pyrite which are at the interface with the calcite gouge and sandstone.

others (1976) for quartz gouge deformed with Westerly granite. Figure 2 presents an example of the planar structures developed in the quartz-anhydrite two-layer gouge deformed at a confining pressure of 100 MPa. The structures develop at an angle of 10 to 20° to the sliding surface, and they **commonly** curve slightly to become asymptotic to the country rock-gouge interface. They have been observed in simulated gouges of granites, carbonates, non-platy silicates, and clays deformed at least at pressures above 30 MPa. The similarities of the geometry of these zones with those described by Riedel (1929) have led us to refer to these as R_1 Riedel shear fractures. Further discussion of the geometry of these features is given in the section on fracture arrays.

Cataclastic deformation of quartz or dolomite gouge results in the reduction of grain size (e.g., Engelder, 1976, 1974). Therefore, the grain size of these minerals could be used as a rough measure of the intensity of gouge deformation. Logan and Shimamoto (1976) analyzed the grain size of deformed dolomite (average initial grain size = 0.088 mm; specimen deformed at 85 MPa pressure) along these R_1 fractures by using SEM photomicrographs. They obtained an average size of 0.5 μm after about 1.4 cm displacement along the sliding surface. This reduction of grain size is in fact remarkable. But the grains are still considerably larger than those at the country rock-gouge interface, which are totally invisible even under much higher magnifications than that used for the analysis of grain size.

The grain size of deformed quartz along the R_1 fractures has been measured from SEM photomicrographs taken at small portions near the center and the surface of the gouge. The grain-size distributions are very similar at the two locations, which suggests a uniform distribution of grain size along the planar zones. The average grain size is 0.7-0.8 μm . This grain-size reduction of quartz is almost comparable to that of dolomite (0.5 μm). In the light of Engelder's (1973, 1974) results, the average grain size along the R_1 fracture is about 4 times larger than that in the gouge at the rock-gouge interface (0.2 μm) and about 30 to 40 times smaller than that in the major portion of gouge (30 μm).

Thus, the data on the grain size of deformed quartz and dolomite indicate that the deformation along the R_1 shear fractures is much more intense than that in the **major** portion of the gouge, but not as intense as that along the country rock-gouge interface. Hence, the **critical** portion of the system which suddenly unlocks at a stick-slip event is perhaps the boundary between the country rock and gouge. **However**, possible roles played by the planar structures cannot be denied only by these data.

In order for the R_1 fractures to be the site of locking of the system, which breaks suddenly at stick-slip, a displacement has to take place along these structures. Observe in Figure 2b that quartz grains with undulatory extinction are displaced along the R_1 fractures. These grains have very similar optical properties, so that they were perhaps a single grain before deformation, but the grain is fractured and displaced along the R_1 fracture during the frictional sliding. This is,

therefore, a direct evidence of displacement along the R_1 within the gouge. However, the amount of displacement is only about 0.2 mm and much smaller than the total amount of displacement of specimen along the precut (1.2 cm). The surface of deformed gouge, especially when the deformation is by violent stick-slip, takes on a very smooth and shiny appearance. On the other hand, the R_1 fractures within the gouge rarely exhibit slickenside surfaces. All of these observations indicate that a certain amount of displacement takes place along these discrete planar structures, but it is much smaller than the displacement at the country rock-gouge interface. The grain size data and the above observations all suggest that the country rock-gouge interfaces, rather than the R_1 fractures within the gouge, are the most likely sites of the critical locking of the system. It should be remarked that the development of R_1 fractures in the gouge cannot necessarily be correlated with the onset of stick-slip, because they form regardless of whether stick-slip occurs or not. Sumners and others (1976) suggested that the oblique shearing in the gouge precedes the sudden slip at a stick-slip event, and hence the microseismic activity along the planar structures in a natural fault zone could be used as a precursor for an earthquake. However, it appears very difficult to correlate the displacements along the R_1 fractures with the onset of sudden slip, because the development of the structures is common in deformed gouges for both stable sliding and stick-slip.

The shift from homogeneous cataclastic flow to heterogeneous deformation concentrated within R_1 fractures and at the interface between the simulated gouge and the country rock occurs within the first few millimeters of displacement for laboratory specimens. This change in behavior is abrupt and is postulated to be a function of the energy necessary to continue grain-size reduction of the entire gouge zone. As the grain size is reduced, the surface area also increases and the energy necessary to continue this reduction increases exponentially (Shimamoto, 1977). It is postulated that this increase in energy precludes further homogeneous deformation of the entire zone, but rather the displacement becomes concentrated along narrower selected sites, in R_1 fractures and at the interface of the gouge and country rock. Although further displacement does involve additional grain size reduction, this would necessitate less energy than if the total volume of the gouge zone were involved. Additionally, at the interface with the grain size reduction, this displacement surface becomes more planar, facilitating further displacement at lower energy levels.

EFFECTS OF TEMPERATURE ON SIMULATED FAULT GOUGE

The description of the history of the simulated fault gouge and the accompanying fracture array just presented are based upon evidence gathered from experiments done at room temperature. In order to more closely simulate conditions within the Earth's crust, experiments at elevated temperatures have been conducted utilizing a simulated gouge of calcite. This material was chosen as a suitable material because (1) its frictional behavior at room temperature already is well documented

(Logan and Shimamoto, 1976; Shimamoto, 1977), (2) it exhibits stick-slip at reasonable laboratory conditions, (3) it is expected to go through the brittle to ductile transition with increasing temperature, possibly making the results applicable to other minerals which might undergo a similar transition.

Compression tests on room-dry specimens were carried out at a constant confining pressure of 200 MPa, $2 \times 10^{-4} \text{ sec}^{-1}$ nominal strain rate, and temperatures to 900°C. For experiments at 250°, 400°, and 600°C axial thermal gradients within the sample do not exceed 25°C. Experiments with temperatures listed as > 400° were made early with an internal furnace that we now realize produced a steeper thermal gradient, so that the true temperature may be as much as 100° greater than the listed value. The experiment designated < 600°C had a furnace dysfunction, but from its stress-strain curve and gouge fabric we believe its temperature must have been between 400° and 600°C and probably closer to 600°C.

Experimental Results

Stress-strain data. The ultimate strength of the calcite gouge decreases with increasing temperature (Figure 4). Moreover, it undergoes a transition from stick-slip to stable sliding between 250° and 400°C. Steady state behavior occurs at about 600°C with pronounced work softening at 900°C. Specific stress-strain behavior is correlated with deformation mechanism and corresponding fabric change below.

Gouge fabric. At room temperature the specimen is characterized by high ultimate strength and large unstable (stick-slip) stress drops of about 200 MPa (Figure 4). Premonitory slip is observed prior to each stress drop. In thin section R₁ and R₂ shears are observed within the gouge layer (Figure 5). The acute angle between R₁ shears and the gouge-rock interface averages 15-20°. These shears occur in all stages of development from incipient zones, to zones of intense grain-size reduction, to discrete fractures with an obvious loss of cohesion. Comparatively short R₂ fractures are developed at about 70-80° to the gouge-host interface. In addition, room temperature gouge layers are characterized by an undirected cataclastic texture of angular clasts randomly arranged within a structureless, finer matrix, similar to that of a typical cataclasite (Higgins, 1971, p. 5-6).

At 250°C, the gouge zone is somewhat weaker but still exhibits stick-slip, although with much smaller stress drops, about 20 MPa. One test however, displayed stable sliding until jacket failure at 4 percent strain. Premonitory slip is not observed, but this is probably a function of the insensitivity of the recording system for small stress drops. In thin section, the texture within the gouge layer essentially is the same as in room temperature specimens, except that there is development of a modest preferred orientation of the long axes of elongate prophyroclasts (Figure 5b). Such clasts are oriented with their long axes oblique to the gouge-rock interface and at high angles to the cylinder axes. R₁ and R₂ shears are developed, but R₁ shears exhibit a wider range of orientation than at room temperature.

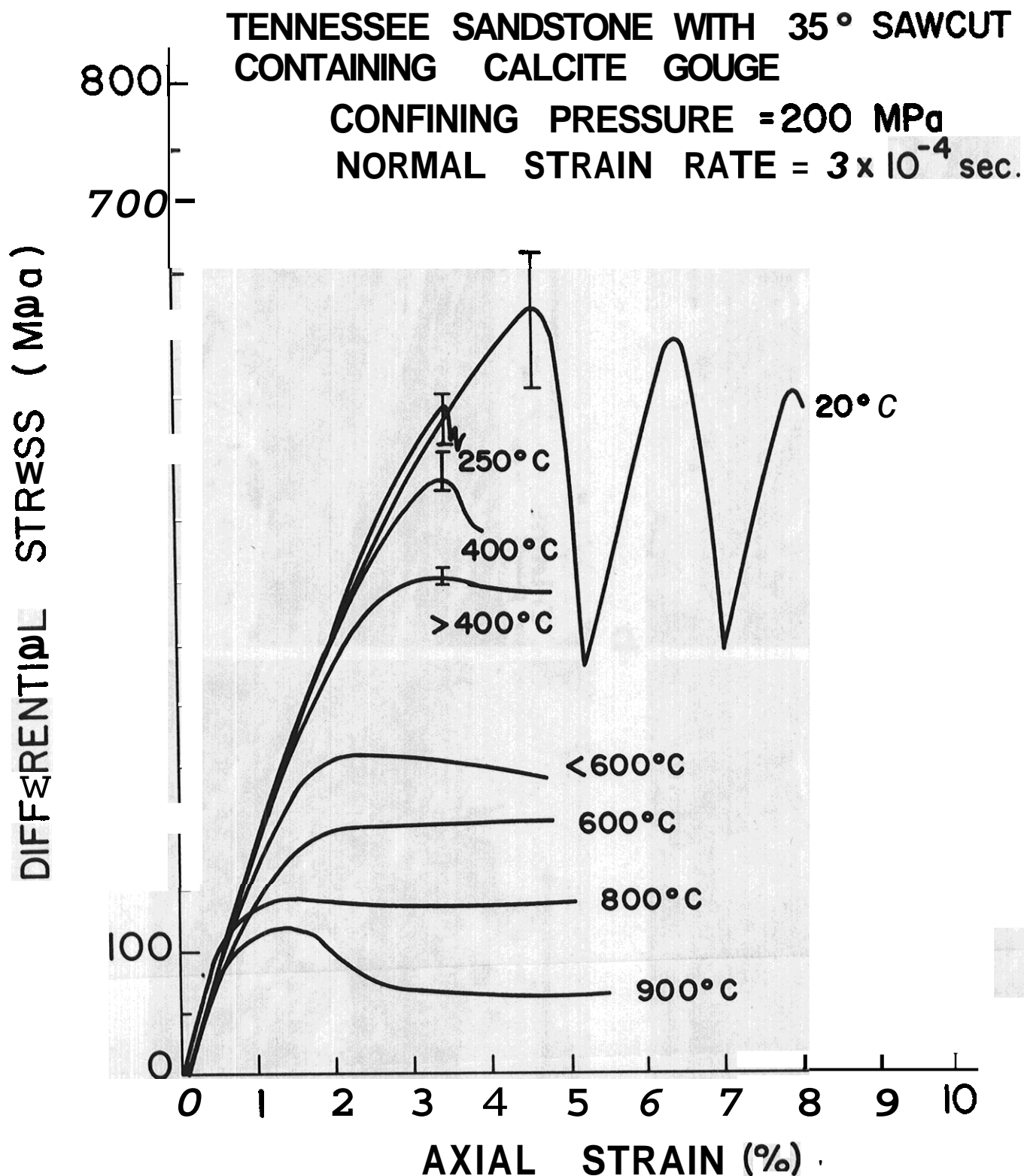
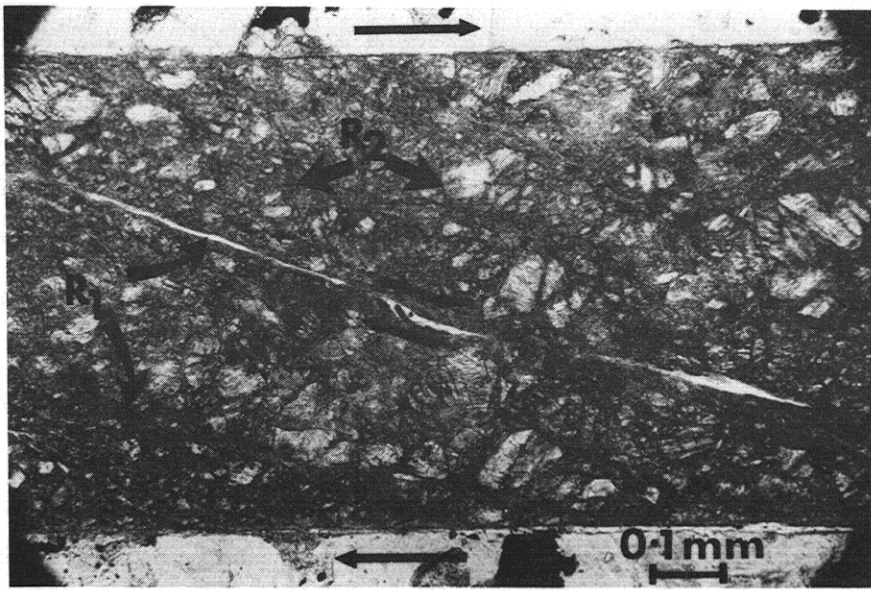
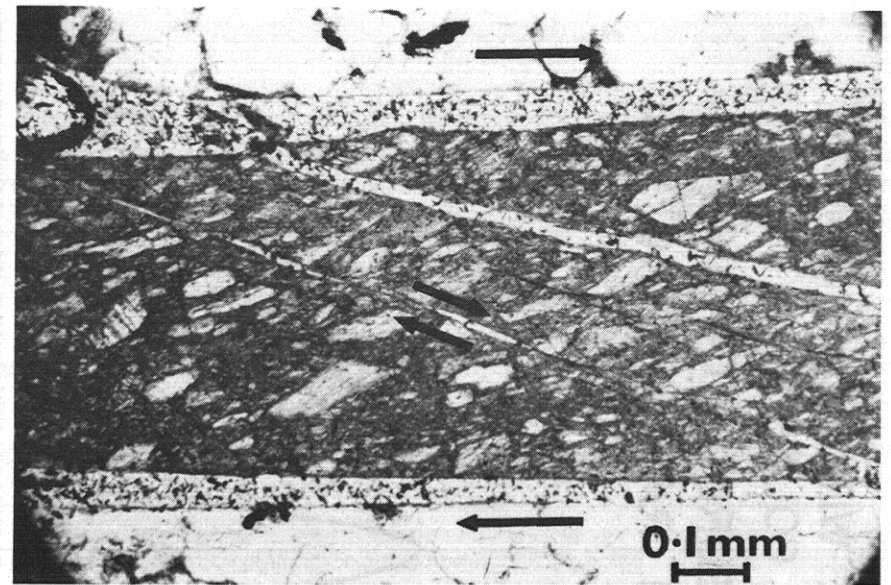


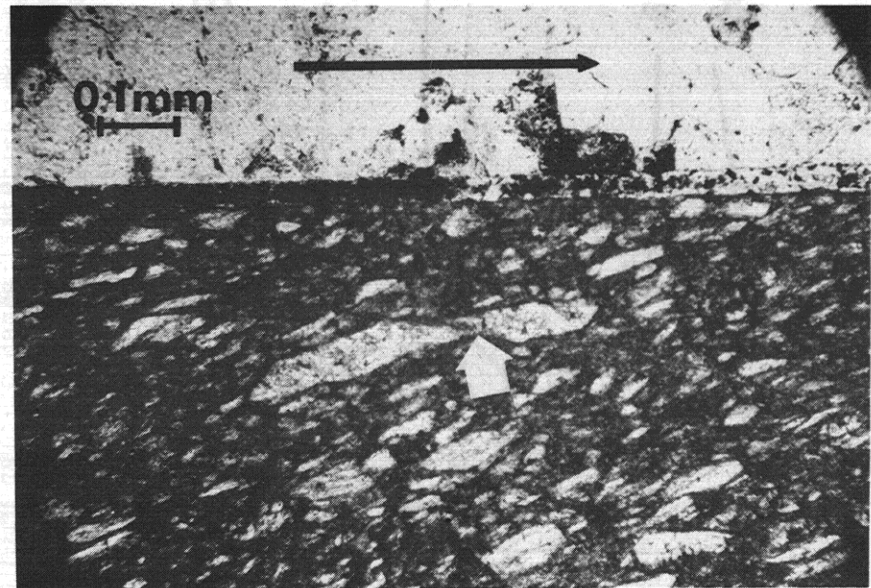
Figure 4. Stress-strain curves show influence of temperature on the frictional strength and sliding mode of 35°-precut specimens of Tennessee sandstone with calcite gouge. Vertical bars indicate the range of maximum differential stress for different tests under the same experimental conditions. See text for a discussion of temperatures.



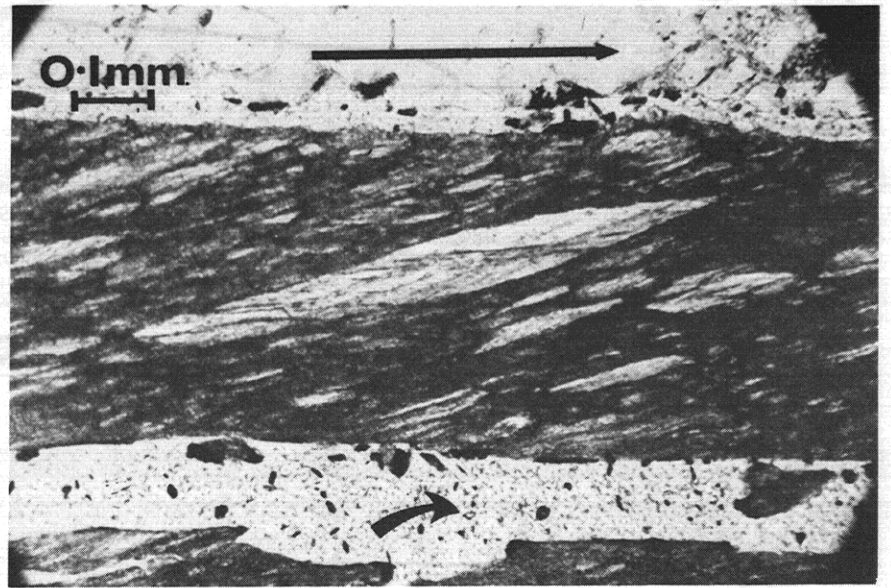
a



b



c



d

Figure 5. Photomicrographs show features of the gouge fabric in (a), room temperature, (b) 250°C, (c) 400°C, and (d) > 400°C. Sense of shear across gouge zone and along R₁ Riedel shears is right-lateral (see straight arrows). Note: R₁ and R₂ are developed in both (a and b); porphyroclasts become progressively elongated with increasing temperature; and R₁ in (c) offsets porphyroclast and is inclined at a smaller angle to the gouge-host rock interface than in (a or b). The curved arrow in (d) marks a zone in which gouge material was plucked during preparation of thin section. Plane polarized light.

At 400°C, the gouge zone is weaker than at 250°C, and the sliding behavior is stable in two out of the three tests carried out at this temperature. The third test displayed stick-slip with small--though audible--stress drops of magnitude about 20 MPa. These differences in mechanical response are very clearly reflected in the microstructure of the deformed gouge layers. Specimens showing stable sliding are characterized by a well developed preferred dimensional orientation of the porphyroclasts (Figure 5c), while the specimen showing stick-slip has only a weak development of this same preferred orientation, similar to that observed in the 250°C test. In both specimens R_1 shears are conspicuous and are inclined at only 8-10° to the gouge-host rock interface. Right-lateral displacement along these shears is marked by offsets of porphyroclasts (Figure 5c). Measurements of these and other offsets indicate that the sum of the displacements along these fractures average about 50 μm for the tests where the total displacement parallel to the sliding surface is 2 mm. This supports our previous contention that most of the displacement is localized at the gouge-rock interface. The gouge thickness is reduced (during the test) from 1 mm to approximately 0.5 mm, although this latter value does vary somewhat from test to test.

At temperatures greater than 400°C, all tests exhibit stable sliding. Between 400° and 500°C, the trend of weakening with increasing temperature is continued, and the microstructure is dominated by an extremely well developed preferred dimensional orientation of the porphyroclasts (Figure 5d), with long axes oriented at 10-20° to the gouge rock interface, and at high angles to the cylinder axis. These porphyroclasts have undergone large strains as evidenced by aspect ratios of 10 and greater, compared with their undeformed ratios which as a rule do not exceed 2. This dimensional fabric is quantitatively represented in an approximate manner in an R_f/ϕ diagram (Dunnet, 1969; Ramsay, 1967) (Figure 6). In addition to the dimensional fabric, the porphyroclasts display a well developed crystallographic preferred orientation as shown in the fabric diagram for [0001] (Figure 7); c -axes are inclined at 10 to 20° to the maximum finite shortening direction. The data, although by no means conclusive, suggest that the principal extension, e_1 , within the shear zone lies at about 17° to the shear zone boundary. Such an orientation for e_1 would be obtained during progressive homogeneous simple shear after a shear strain, γ , of 3.0. The calculated shear strain for the test, based on the displacement record corrected for machine and specimen stiffnesses, is 2.72. This indicates that virtually all the shear displacement induced by the test is absorbed in quasi-homogeneous deformation of the calcite layer. In turn, this implies that deformation is not localized at the gouge-rock interface during ductile shearing of calcite gouge, in contrast to the lower temperature behavior previously outlined. Thus, we would expect a difference in the relative width of fault zones of similar compositions depending upon the mechanisms of deformation. Under shallow conditions, where fracture and cataclasis are the dominant mechanisms we would expect the zone of active displacement to occur within only a portion of the total gouge zone width. In contrast, when deeper conditions are encountered where ductile behavior is dominant, we would predict involvement of the total width of the fault zone during displacement.

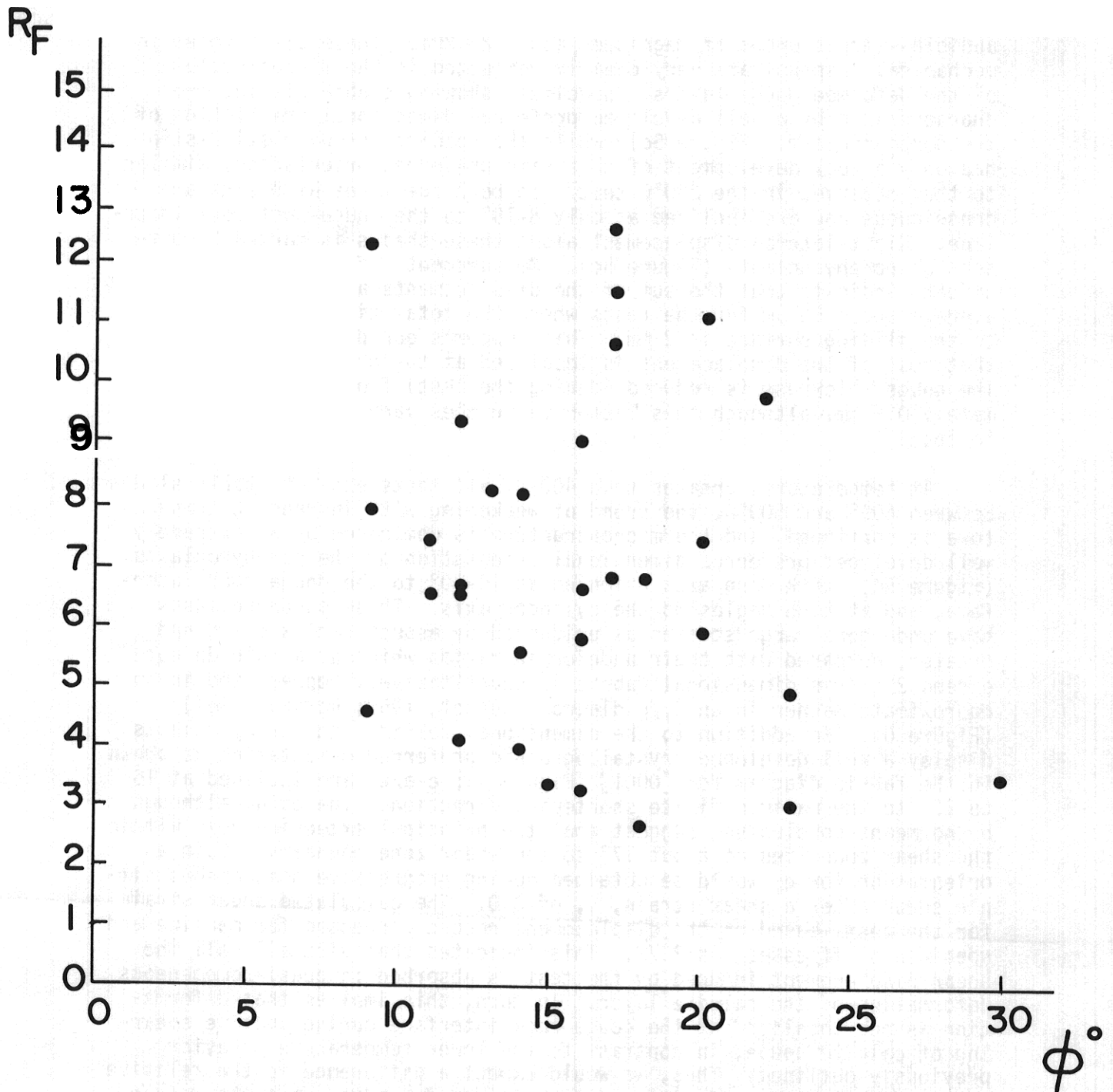


Figure 6. Diagram shows nature of preferred dimensional orientation of calcite porphyroclasts, shortened 5 percent at $> 400^\circ\text{C}$. R_f is the ratio of apparent long to short dimensional axis of each porphyroclast as observed in thin section. ϕ is the angle between the apparent long axis of the clast and the gouge-host-rock interface.

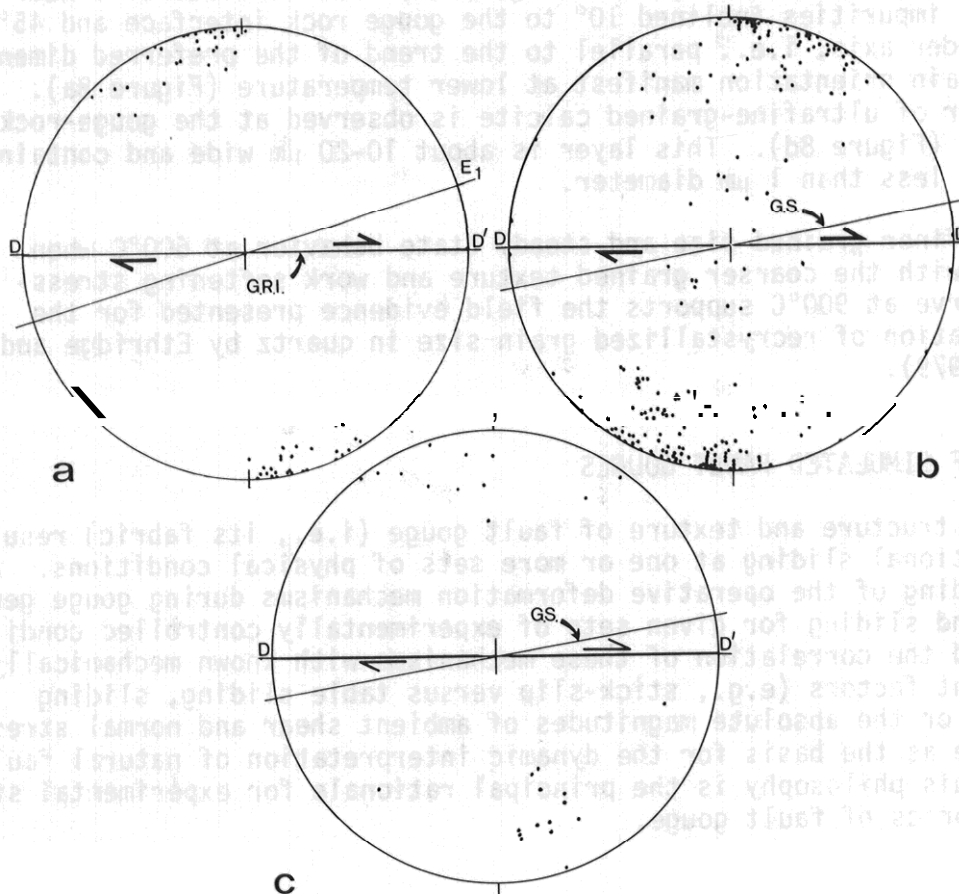


Figure 7. Diagrams show nature of crystallographic orientation in deformed calcite gouge. The plane of each diagram is perpendicular to the gouge-host-rock interface (G.R.I.), and contains the displacement direction OD' . Right-lateral sense of shear is indicated. Data are plotted in lower-hemisphere, equal-area projection. (a) $> 400^\circ\text{C}$, data are 57 c-axes in markedly elongated porphyroclasts. Average axis of elongation (E_1) is estimated from Figure 6. (b) 900°C , data are 211 c-axes from recrystallized grains (Figure 8c). Orientation of ghost structure (G.S.) is shown. (c) 900°C , data are normals to 27 $\{10\bar{1}1\}$ planes obtained graphically from twinned grains in (b). Orientation of ghost structure (G.S.) also is shown.

At temperatures approaching 600°C, the gouge layer becomes dramatically weaker and in thin section the well-developed dimensional preferred orientation of the porphyroclasts is still observed, except in isolated patches where incipient recrystallization to an average 3 µm grain size (Figure 8b). At 900°C, the gouge is further weakened, and displays a coarsely-recrystallized, equigranular texture with grains ranging in size from 20-100 µm (Figure 8c). These grains display a strong crystallographic preferred orientation, as demonstrated by the fabric diagram for [0001] and for [10 $\bar{1}$ 1] (Figure 7c). In addition, a "ghost" structure is observed within the recrystallized grains (Figure 8c) that consists of linear trails of impurities inclined 10° to the gouge rock interface and 45° to the cylinder axis, i.e., parallel to the trend of the preferred dimensional grain orientation manifest at lower temperature (Figure 8a). A thin layer of ultrafine-grained calcite is observed at the gouge-rock interface (Figure 8d). This layer is about 10-20 µm wide and contains grains of less than 1 µm diameter.

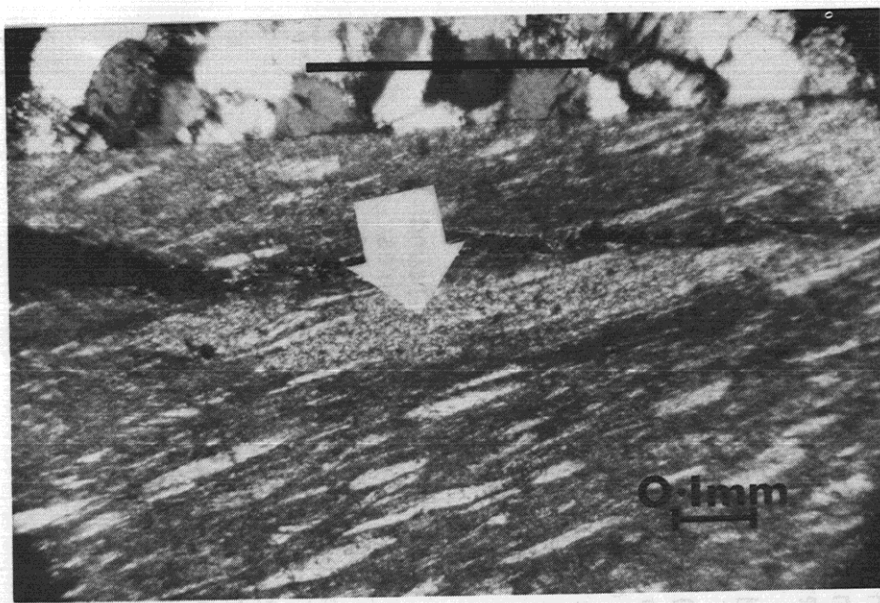
The finer grained size and steady state behavior at 600°C when compared with the coarser grained texture and work softening stress-strain curve at 900°C supports the field evidence presented for the interpretation of recrystallized grain size in quartz by Ethridge and Wilkie (1979).

FABRICS OF SIMULATED FAULT GOUGES

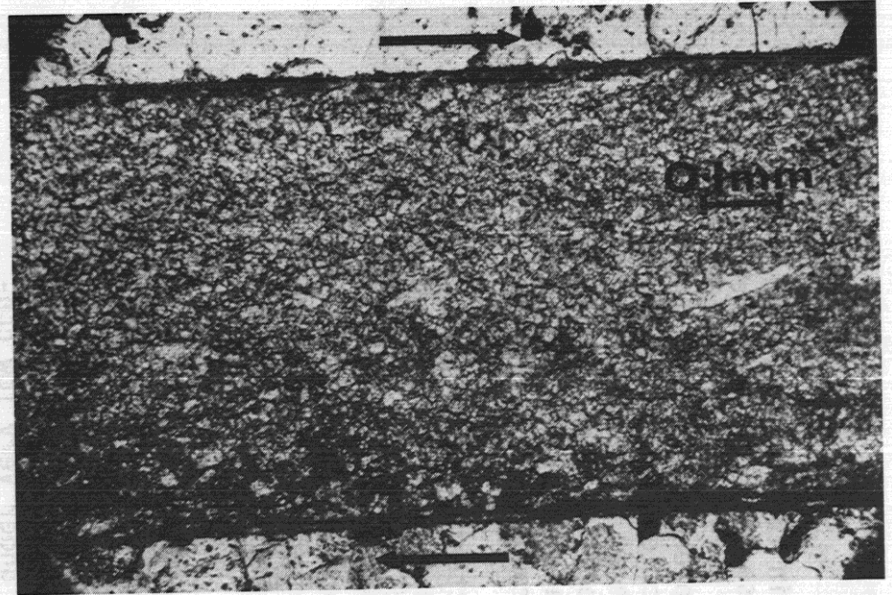
The structure and texture of fault gouge (i.e., its fabric) results from frictional sliding at one or more sets of physical conditions. An understanding of the operative deformation mechanisms during gouge generation and sliding for given sets of experimentally controlled conditions, and the correlation of these mechanisms with known mechanically significant factors (e.g., stick-slip versus table sliding, sliding friction, or the absolute magnitudes of ambient shear and normal stress, etc) serve as the basis for the dynamic interpretation of natural fault gouge. This philosophy is the principal rationale for experimental study of the fabrics of fault gouge.

Fracture Patterns in Gouge

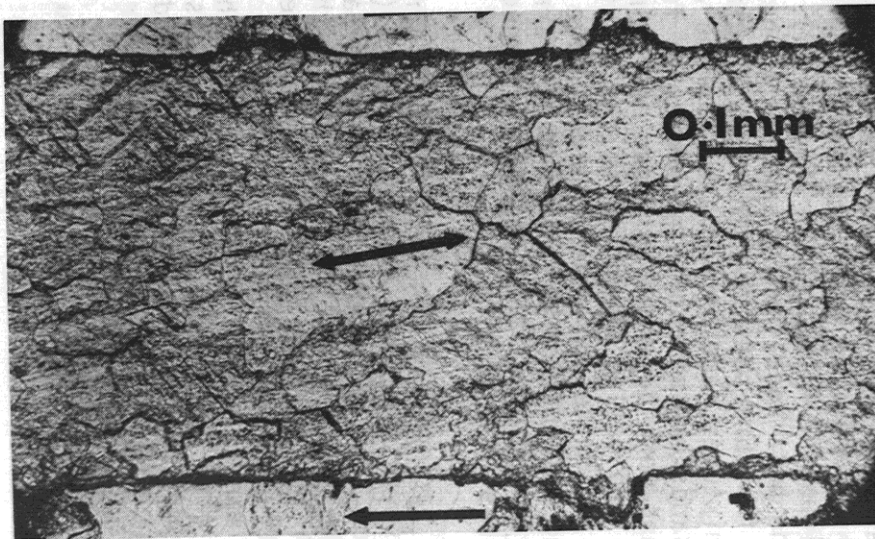
Fractures in or immediately adjacent to fault zones, formed as a consequence of shear displacement along the primary fault, have long been recognized and studied (e.g., Cloos, 1928; Riedel, 1929; Cloos, 1932, 1955; Oertel, 1965; Morgenstern and Tchalenko, 1967; Brown and Vedder, 1967; Wallace and Roth, 1967; Roering, 1968; Lajtai, 1969; Tchalenko, 1970; Tchalenko and Ambraseys, 1970; Wallace, 1973; Jaeger and Gay, 1974; Freund, 1974; Engelder, 1974; Jackson and Dunn, 1974; Conrad and Friedman, 1976; Logan and Shimamoto, 1976; Shimamoto, 1977; and Byerlee et al., 1978). Of particular interest are the patterns of en echelon shears and tensile fractures that are developed along the surface trace of major faults such as the San Andreas (Allen and Smith, 1966; Brown and Vedder, 1967; Wallace and Roth, 1967; and Wallace, 1973) and the Dasht-e-Bayas earthquake zone in Iran (Tchalenko and Ambraseys, 1970). Work along the San Andreas has indicated that the R₁ Riedel shear



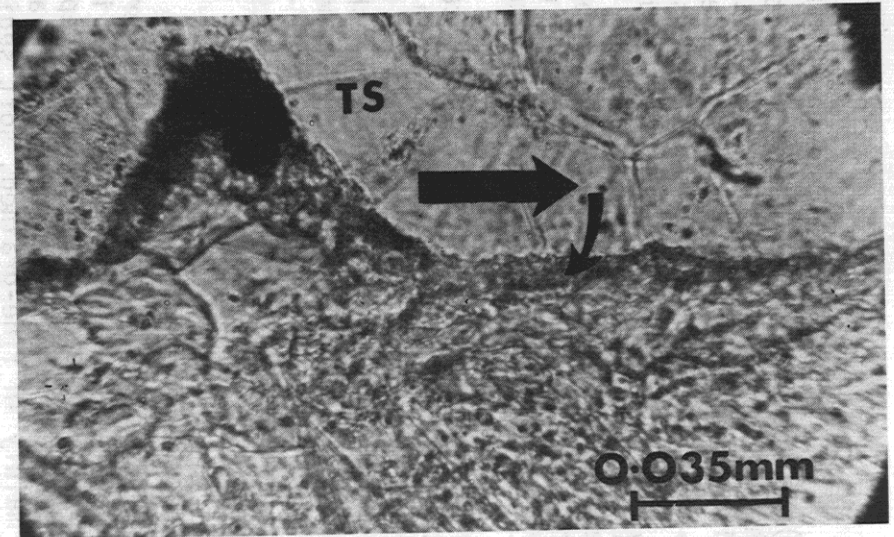
a



b



c



d

Figure 8. Photomicrographs show features of gouge fabric (a) $< 600^{\circ}\text{C}$, (b) 600°C , and (c and d) 900°C . Sense of shear across gouge zone is right-lateral as indicated by straight arrows. Note: highly elongated porphyroclasts and zone of incipient recrystallization (bold white arrow) in (a); fine-grained, recrystallized mosaic with ghost of R1 in (b); coarser, equidimensional recrystallized crystals in (c) with ghost structure (double ended arrow) parallel to trend of former elongated porphyroclasts; and in (d) very-fine-grained calcite fills indentation of gouge into a hole in the Tennessee sandstone (TS) at the gouge-host-rock interface. Plane polarized light.

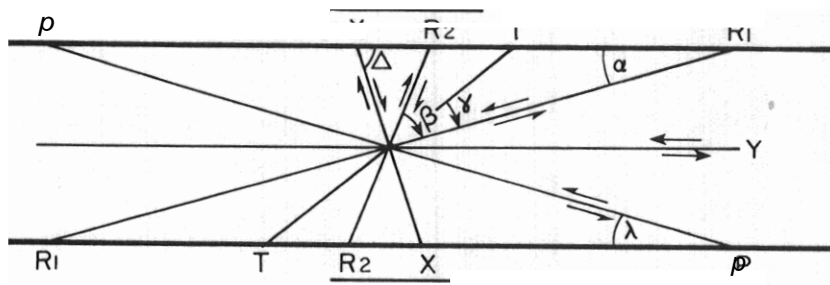
(Figure 9a) is the best developed with fractures in the P orientation and sense of shear also present (Wallace, 1973). These tectonic fractures are significant because (1) they begin to develop prior to the actual earthquake, and therefore are potentially useful precursive events (Allen and Smith, 1966); (2) displacement rates and directions can be recovered from them (Wallace and Roth, 1967); (3) the length of the zone in which they are developed is about that of the deepest foci (Wallace, 1973); and (4) they are associated with earthquakes of moderate magnitude (5.0-7.0) and are relatively uncommon for smaller quakes (Brown and Vedder, 1967).

Tchalenko and Ambraseys (1970, p. 43) call attention to another significant aspect of these fractures. From the angles between R_1 and P to the shear zone, the assumption that σ_1 is inclined at 45° to the shear zone boundary, and the view that the shear fractures can be explained by the Coulomb failure criterion, these workers inferred an angle of internal friction (ϕ) of 35° to 40°--a value not unreasonable for the type of materials (colluvial deposits and clayey silts) in which the fractures were developed.

This aspect of the work did not receive as much attention as perhaps it deserves because the fracture patterns were developed in unconsolidated sediments at the Earth's surface. That is, it is not known whether such fractures are pervasive of fault zones at depth. Indeed, the whole array of Riedel shears and other "second order" fractures have been observed and studied mainly in fine-grained, soft sediments under very low confining pressures. Until recently their development under high confining pressure (> 50 MPa) has been limited to the recognition of the conspicuously developed R_1 Riedel shear (Figure 2a). Recently our experimental study of the host-rock-fault gouge system has led to the recognition of a six-fold fracture pattern within gouges composed of quartz, quartz and anhydrite mixtures, and orthoclase deformed along 35°-precut surfaces of Tennessee sandstone at confining pressures from 50 to 350 MPa (Figure 9). The specimens were deformed by Logan and Shimamoto (1976), and by Shimamoto (1977) who called attention to the existence of the R_1 shears. Gouges of calcite, dolomite and other minerals have not as yet been examined in detail. The recognition of this fracture array is made possible by use of a blue-stained epoxy that faithfully preserves the pattern and makes it conspicuous microscopically.

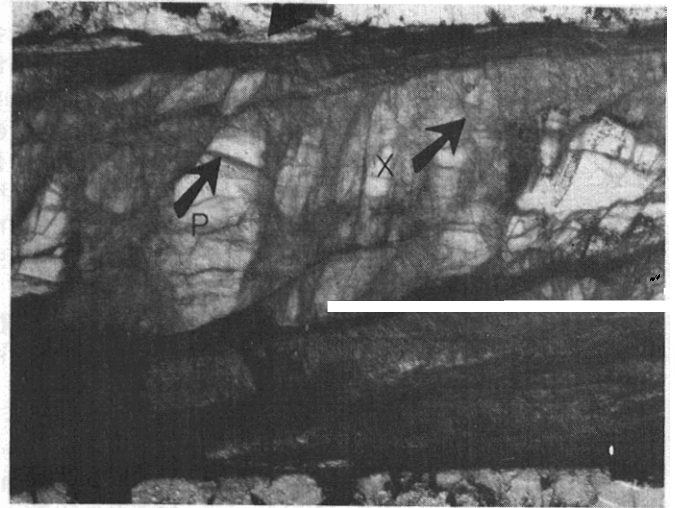
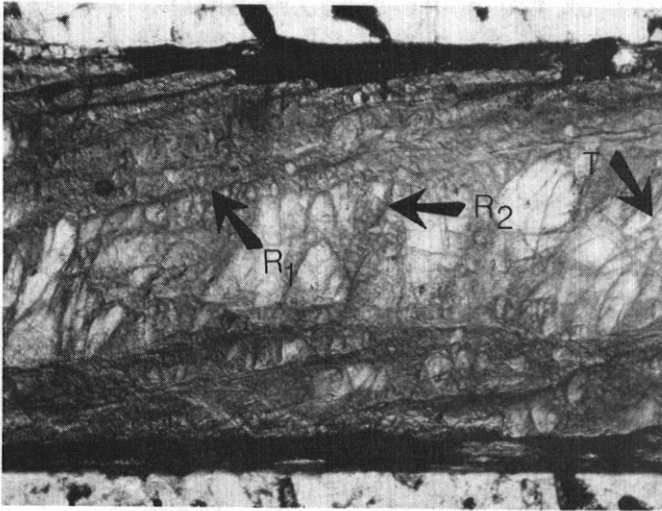
All or part of the six fold fracture array (Figure 9a) has been found in each of seven specimens examined to date (Table 2). All the fractures have a common line of intersection that is parallel to the shear zone and at 90° to the shear direction. Therefore, their traces in a thin section cut parallel to the shear direction and perpendicular to the shear zone give their true angles of intersection. The angles α , β , γ , Δ , and Λ were measured in many fields of view along each shear zone (Table 2) and averaged to give the values in Table 2. Sets R_1 , R_2 , T, and P have been found by other workers, notably Tchalenko and Ambraseys (1970) in the Dasht-e-Bayas fault zone. We note that their average R_1 A P is 32°, and the average experimental value is 31° their average R_1 A R_2 is 50° to 57°, ours is 53°; their R_1 A shear zone (α) is 15 to 20°, our is 15°.

Figure 9. Geometry and photomicrographs of the gouge-fracture-array. (a) Drawing shows orientation of fracture sets R_1 , R_2 , T, X, P, and Y developed within gouge relative to the overall left-lateral sense of shear for the gouge-host-rock system. Angles α , β , γ , A , and λ are the averages from Table 2. Photomicrographs (b-e) show development of this fracture array in specimen TQG4, a quartz gouge deformed at 250 MPa. Each photomicrograph is oriented parallel to the line-drawing, and the arrows point to different fracture sets within the six-fold array so that the unmarked fractures can be identified readily by correlation with (a). A small part of the host rock (Tennessee sandstone) is visible at the boundary of the gouge in (b, c, and d). Of special interest note: (1) fractures are very conspicuous in these photomicrographs because the blue-stain-epoxy used to impregnate the gouge enhances their contrast, especially in plane polarized light (b, c, and d); (2) R_1 is the best developed of the fracture sets, and it tends to curve asymptotically into the host-rock interface; (3) immediately at this interface the planar anisotropy in the gouge is parallel to the interface and glass is developed at places (see arrow labeled G in [c], glass also visible in [b and d]); (4) left-lateral sense of shear is obvious for R_1 (see straight long arrow in [e]), and for P as indicated by the microscopic feather fractures in (d) (Conrad and Friedman, 1976); and (5) fracture set T is poorly documented in these photographs. Scale line corresponds to 0.5 mm in (b and c) and 0.13 mm in (d and e). Only (e) is photographed in cross-polarized light.



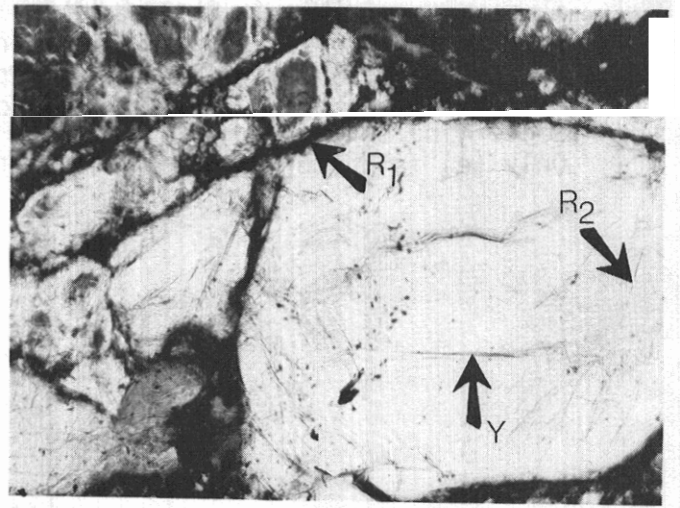
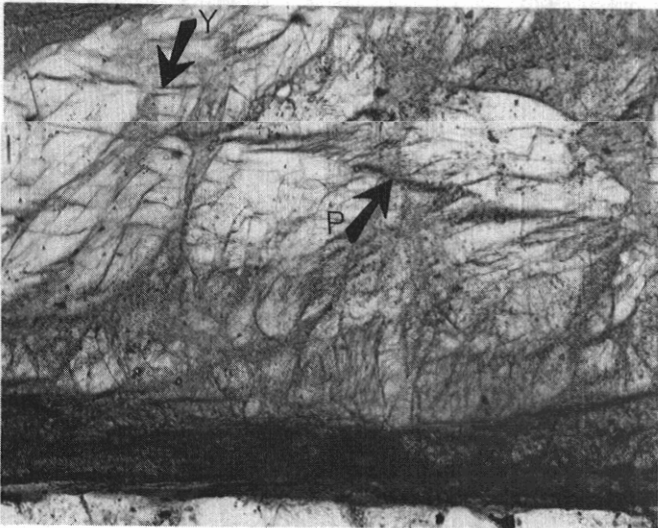
θ

ϵ



b

c



d

e

Table 2. Angular Relations Among Gouge Fractures in Seven Specimens¹

Specimen	Gouge Composition ²	Pc (MPa)	Average Angles (degrees) ³					Relative Fracture Development ⁴
			α	β	γ	A	λ	
TQG3	100% Q	50	17	55	22	70	17	R ₁ , R ₂ , P, T, X ⁵
TQCG6	95% Q, 5% A	100	14	52	20	76	18	R ₁ , R ₂ , P, T, X
TQG4	100% Q	250	18	53	28	72	19	R ₁ , R ₂ , X, P, T
TQCG7	85% Q, 15% A	100	18	53	26	74	19	R ₁ , R ₂ , X, P, T
TQCG5	25% Q, 75% A	100	16	57	-	71	18	R ₁ , X, R ₂ , P, T
TOG1	100% O	100	12	50	19	69	9	R ₁ , R ₂ , X, P, T
TOG4	100% O	300	13	52	-	74	15	R ₁ , R ₂ , P, X, T
Overall Averages: (Figure 9a)			15	53	23	72	16	

1. Specimens are 35"-precut cylinders of Tennessee sandstone with 1 mm thick gouge deformed dry, at room temperature and at a shortening rate of $(2-10) \times 10^{-4}/\text{sec}$ (Shimamoto, 1977).
2. Q is for quartz, A is for anhydrite, and O is for orthoclase.
3. For definition of angles see Figure 9a.
4. Listed left to right in order of decreasing abundance.
5. Fracture sets all in incipient stage of development in specimen TQG3.

Table 3. Comparison of Average $\tan \phi$ from Gouge Fracture Array and From Experimental Data

Specimen	Average $\tan \phi$ From Fractures	$\tan \phi$ Calculated from Ultimate Strength Data	Fracture Data Giving Best Fit
TQG3	.67	.66	P (λ angle)
TQCG6	.67	.68	P (λ)
TQG4	.72	.70	R ₁ (α)
TQCG7	.77	.68	R ₁ (α)
TQCG5	.66	.70	P (λ)
TOG1	.72	.70	R ₁ \wedge R ₂ (β)
TOG4	.62	.70	R ₁ \wedge R ₂ (β)
Averages:	.69	.69	

Fracture set X (Figure 9) has not been recognized previously and set Y has largely been taken for granted in that it parallels the major shear zone and has been reported by others (Mandl et al., 1977). We note that there are some differences in the relative abundances of these fractures and in their angular relations with gouge type and confining pressure (Table 2).

Mechanical Significance

Following the logic of Riedel (1929) and Tchalenko and Ambraseys (1970) which assumes the Coulomb fracture criterion holds, and that σ_1 is inclined at 45° to the gouge-host-rock interface, four angular relations are recognized that permit determination of the angle of internal friction (ϕ) as follows (Table 3).

$$\begin{array}{l} \bar{R}_1 \wedge \bar{S} \text{ Shear Zone} = \alpha = \phi/2 \\ \angle P \wedge \bar{S} \text{ Shear Zone} = \lambda = \phi/2 \\ \angle \bar{R}_1 \wedge \bar{R}_2 = \beta = 90 - \phi \\ \angle T \wedge \bar{R}_1 = \gamma = 45 - \phi/2. \end{array}$$

Using the angles in Table 2 and the above relations, the average $\tan \phi$ was calculated for each of the seven specimens (Table 3, column 2). Then $\tan \phi$ was calculated using the ultimate strength for each specimen from Shimamoto (1977) as a basis of comparison (Table 3, column 3). Finally, in Table 3 (column 4) we list the angle that gives the best fit to the experimental data. Clearly, the agreement in $\tan \phi$ is reasonably good. In addition, from Engelder (1973, p. 66) the coefficient of internal friction for quartz gouge is 0.70 at a confining pressure of 50 MPa; and Shimamoto (1977, p. 112) shows that the coefficient of sliding friction for quartz and orthoclase gouges is 0.70. The overall agreement among these data suggest that the gouge-fracture-array may be a significant petrofabric tool from which a mechanically significant parameter (coefficient of friction) can be recovered.

This same reasoning may be applied to explain why R1 shears tend to curve asymptotically into the gouge-host-rock-boundary (Figure 9b, c, and d). That is, the gouge at this boundary is mechanically behaving more ductily than further away within the gouge. This behavior would correlate with the concentration of slip at the boundary and the corresponding development of the very-fine-grained gouge there.

Limitations

Now, we recognize that there may be severe limitations to the usefulness of the gouge-fracture-array as outlined above. For examples:

1) In principle, from the fracture array one can infer the magnitude of the coefficient of internal friction. Is this coefficient equal to the coefficient of sliding friction in fault zones as it appears to be

in the experiments (Table 3)? The two are probably the same if the gouge lacks cohesion, i.e., τ_0 is zero, but it is argued that in our experiments this is probably not true.

2) Experimentally it is possible to study specimens for which the total displacement is a few centimeters at most. Moreover, it is recognized that even during this small displacement, deformation first occurs within the gouge and then becomes concentrated along a thin zone at the gouge-host rock interface. What then is the significance of the fracture pattern within the gouge? Is it a feature developed only during initial displacement? Information on the en echelon R₁ and P fractures developed in conjunction with the Parkfield-Chalome earthquakes of 1966 suggests, however, that at least at the surface, these fractures developed before, during and after the main seismic activity, i.e., throughout the displacement history.

3) There may be such a narrow range of $\tan \phi$ values in gouge (or coefficients of sliding friction, for that matter) that the general acceptance of an average value of .6 to .7 may be sufficient for most practical purposes. On the other hand, the facts that experimental values vary from 0.4 to > 0.8, and that a value of 0.81 was used for the Weber Sandstone at the Rangely Anticline (Raleigh et al., 1972, p. 281) suggest that the range of $\tan \phi$ for natural faulting may be large enough to need refinement.

4) The correlation between $\tan \phi$ values described above (Table 3) is based on using the ultimate strength to calculate τ and σ_n on the 35°-precut and hence the coefficient of sliding friction μ_k . Had the initial yield stress or a work-softened residual stress been used the good correlation would have vanished. The point here is that there is a question as to how to correlate the stress-strain record of an experiment with a natural seismically active faulting event (Logan, 1975, p. 360).

FIELD STUDIES

The field occurrences to be considered are two shear zones, which are believed to show different stages of shear zone development and, one gouge zone from the Motagua Fault zone. For purposes of discussion, a shear zone is defined as a tabular zone of rock that has been crushed and brecciated due to shear strain and, following Higgins (1971) a gouge zone is defined as "pastelike material formed by crushing and grinding along a fault. Most individual fragments are too small to be visible by the naked eye, and fragments larger than the average groundmass grains make up less than 30% of the rock."

Figure 10 is a shear zone in serpentinite from the Motagua Fault zone where the length of the exposed zone is about 50 meters and the height about 8-10 meters. Faults labeled A and B are considered here as the primary faults forming the shear zone boundaries and the general sense of shear is left lateral. No displacement markers are visible to

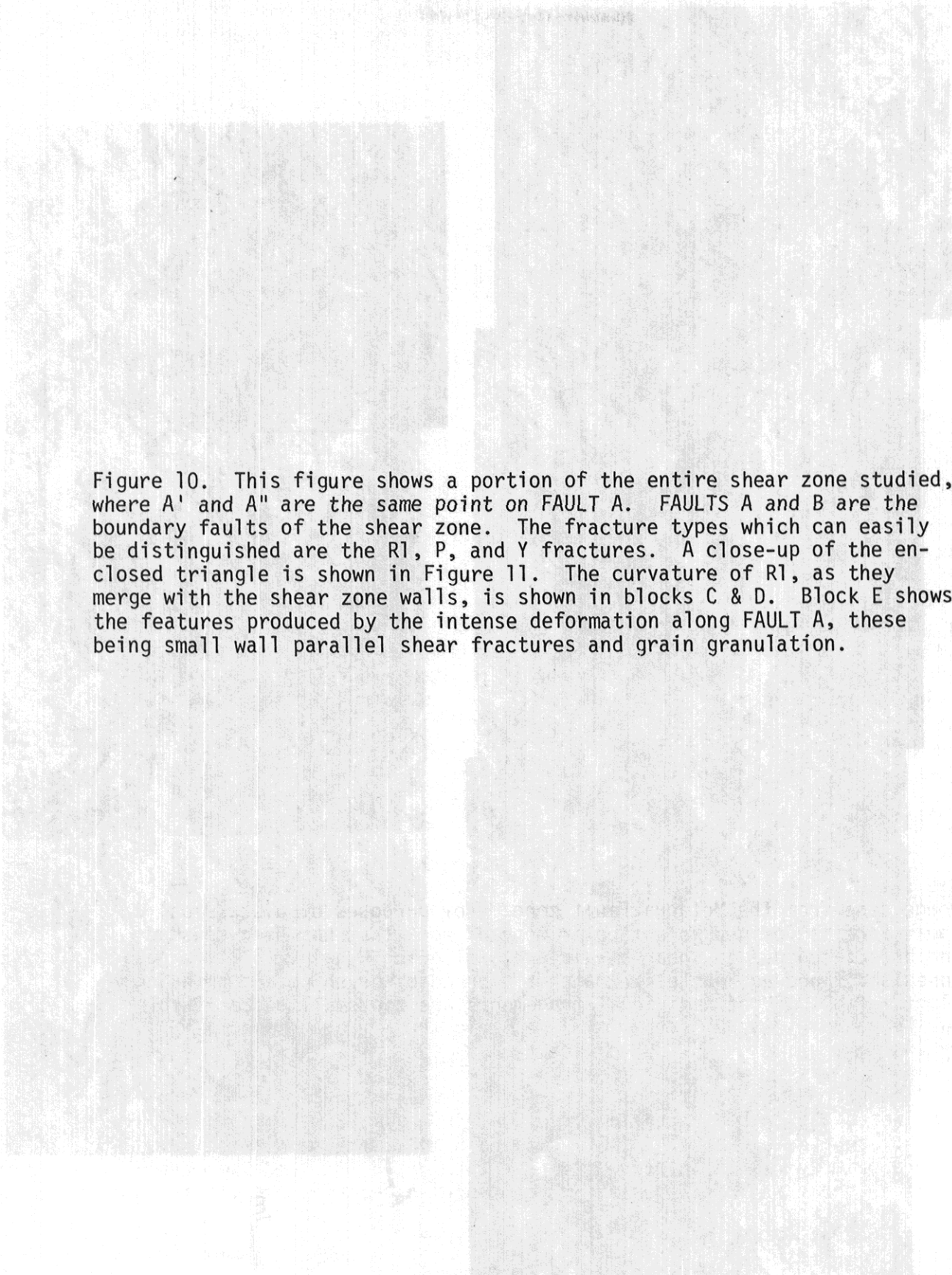
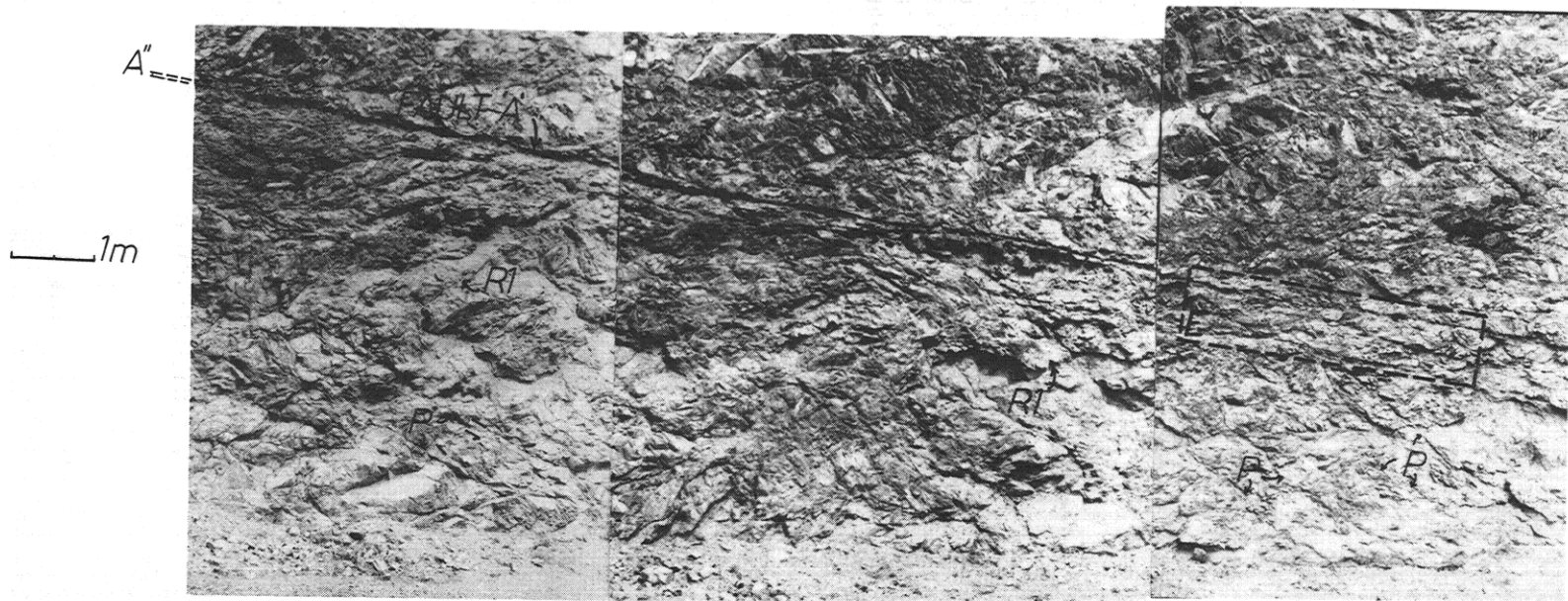
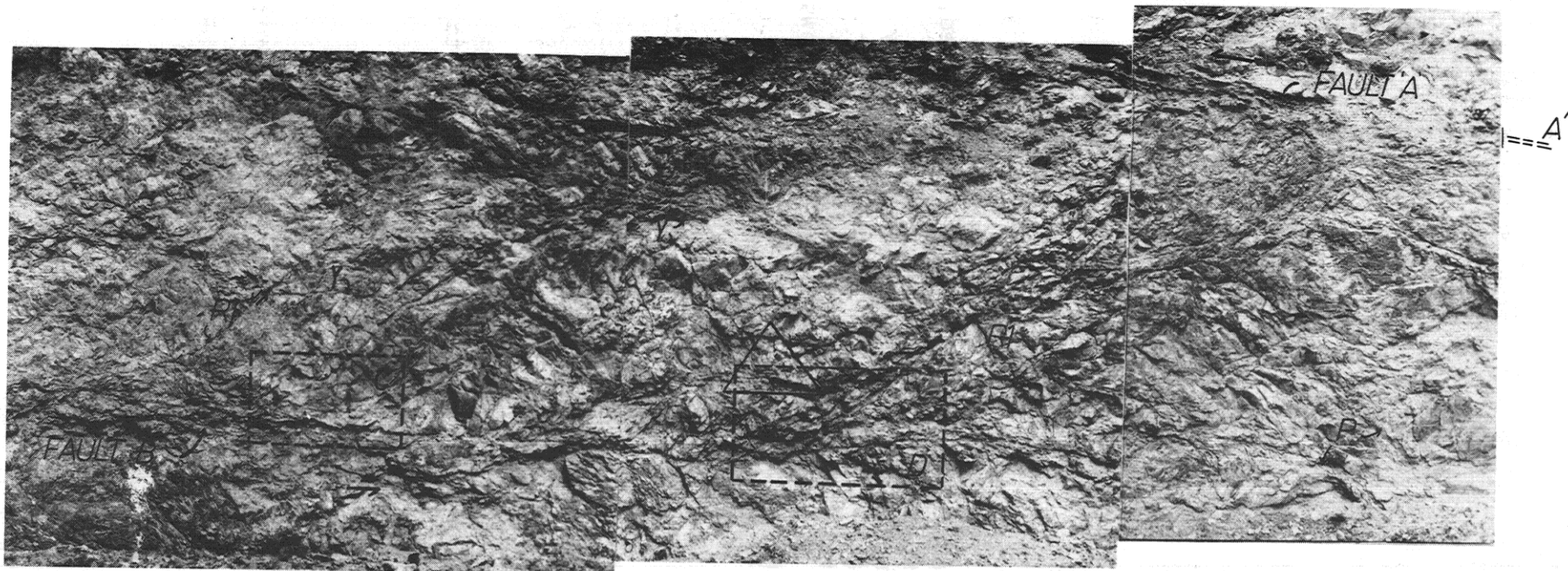


Figure 10. This figure shows a portion of the entire shear zone studied, where A' and A'' are the same point on FAULT A. FAULTS A and B are the boundary faults of the shear zone. The fracture types which can easily be distinguished are the R1, P, and Y fractures. A close-up of the enclosed triangle is shown in Figure 11. The curvature of R1, as they merge with the shear zone walls, is shown in blocks C & D. Block E shows the features produced by the intense deformation along FAULT A, these being small wall parallel shear fractures and grain granulation.



indicate the amount of offset, nevertheless the overall sense of shear can be determined from minor drag effects observed at the margins of the shear zone. Extensive deformation, manifested mainly as granulation and crushing of material, can be seen at the shear zone margins. Fault A (Figure 11) has several smaller parallel shears in its vicinity, forming here what could be considered a true gouge layer as previously defined.

The fracture pattern which has been identified is the following:

1. Conjugate Riedel shears (R1 and R2), shown in Figures 10 and 11. The R1 fractures are pervasive and better developed than the R2 shears. The sense of shear for both fractures is consistent with that described by Riedel (1929), McKinstry (1953), Tchalenko and Ambraseys (1970), and found in our experimental studies. The R1 fractures extend into the fault zone from both its margins, but are truncated in the middle of the shear zone, as are all other fractures, by a fracture parallel to the primary faults. This latter fracture is similar to the Y fracture found in the experimental studies (Figure 9). The geometry of the R1 is sigmoidal, curving asymptotically into the main faults at an angle of about 15-18°. Away from the shear zone margins they steepen to a maximum measured angle of 36°. Granulation of material is present along the R1 fractures (see Figure 11), yet in most cases there is no evidence of macroscopic displacement. Also, there is a "fanning out" of the R1 fractures as they merge with the shear zone boundaries and this can best be seen in the enclosed block D in Figure 10.

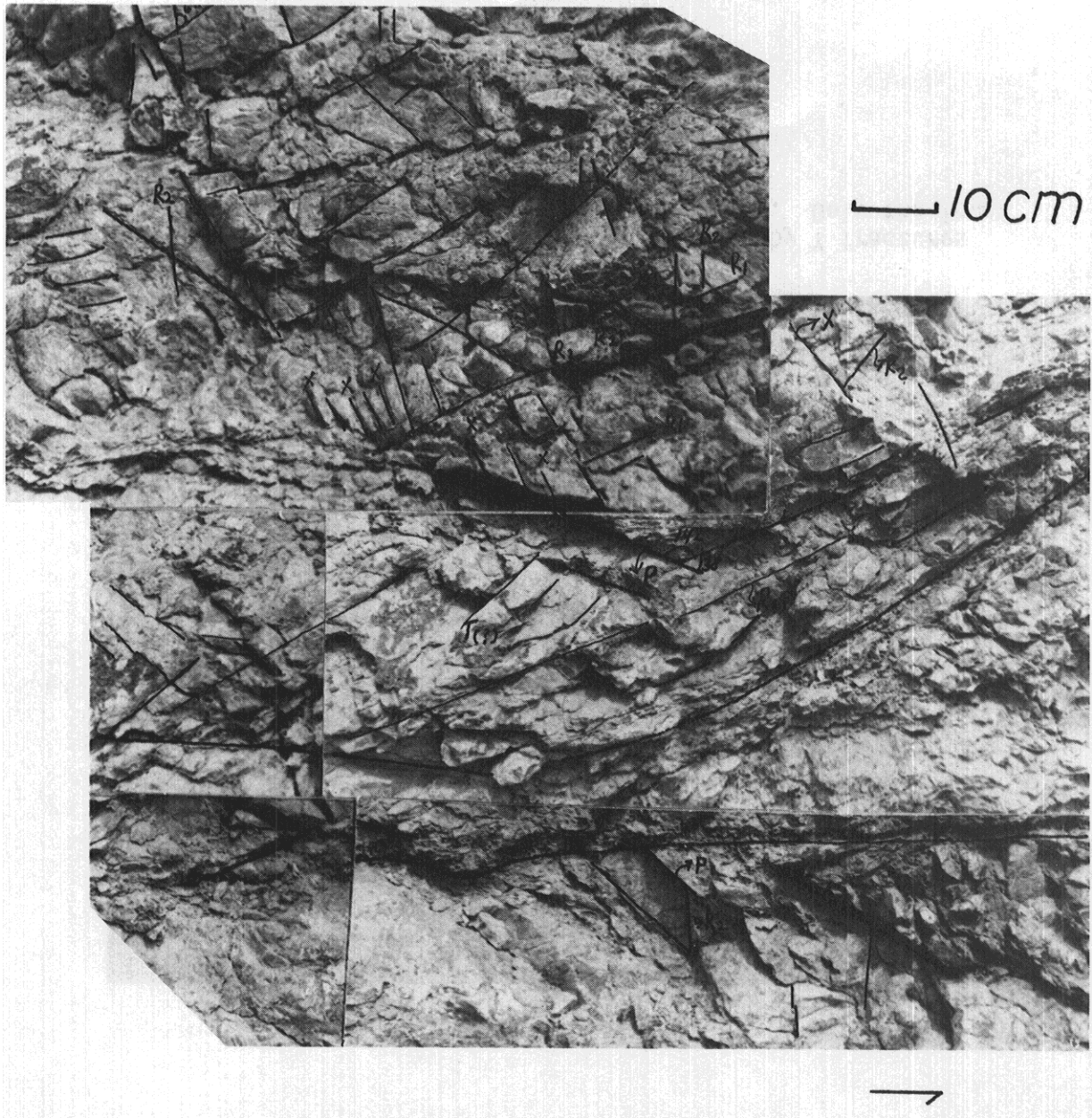
The R2 fractures (see best in Figure 11) maintain linearity throughout their extent. The dihedral angle between R1 and R2 has an average of 60°-70°, which is about 10° higher than what is reported for the experimentally produced Riedel shears in quartz or orthoclase gouge (Table 2).

2. P fractures, shown in Figure 10 and 11, have the opposite sense of shear to the Riedel shears, forming an angle of intersection with the shear zone boundary faults of about 20°. P, like the R2 fractures, maintain their linearity across the fault zone. The angle between P and R1 averages about 38°, where the experimentally measured angle averages about 36°. Granulation of material along P fractures is less than that of R1, and again, evidence for macroscopic displacement is difficult to find.

3. X fractures (Figure 11), form at about 90° to the R1 and no definite sense of shear could be identified.

4. Y fractures (Figures 10 and 12). parallel the trend of the shear zone boundary faults. They are pervasive in the vicinity of fault A and in the middle of the shear zone, in Figure 10 and throughout all the zone in Figure 12. The sense of shear of the Y fracture is consistent with that reported by Mandl et al. (1977) as well as reported in the discussion of the experimentally deformed specimens.

Figure 11. Closeup of area enclosed in triangle in Figure 10. R1, R2, P, and X fractures are indicated. Upper part of figure shows anticlinal steps, formed by intersection of X and R1 fractures. The grain size reduction can be observed along the large RL and P fractures. A possible T fracture orientation is shown in the center of the figure (labeled with a T(?)).





└─ 1m

Figure 12. Shear zone with dominant fabric produced by Y fractures parallel to sub-parallel to the shear zone boundaries. Only the lower boundary fault is shown.

Figure 12 is included to illustrate what may possibly be a shear zone in a different stage of development than that shown in Figure 10. This shear zone, which has dimensions similar to those given for Figure 10, is one of four morphologically similar zones that were studied. The fabric of the shear zone is dominated by Y type fractures, those being the ones parallel to the trend of the boundary faults. The Y fractures are pervasive and range in scale from a few centimeters to a length equal to that of the exposed zone. No other type of fracture is dominant, although there may be R1 and P fractures which are rotated such that they are sub-parallel to the trend of the zone.

The field studies have also concentrated on studying the fracture array associated with gouge zones proper of which Figure 13 is an example. Here the R1, P and Y fractures have been identified with certainty. Severe grain reduction at the gouge-country rock interface masks the junction between the country rock and the observed fractures. The upper portion of the figure shows a "diamond" bounded by intersecting R1 and P fractures, and the angle between these fractures agrees well with that between R1 and P obtained experimentally. Nevertheless, their orientation with respect to the fault indicates that they have undergone some rotation.

DISCUSSION

The previous discussion provides some aspects of the laboratory studies of simulated fault gouge. Additional work is in progress to determine (1) the influence of temperature on dry and saturated simulated gouges containing clays; (2) the significance of irregular fracture interfaces on the simulated gouge behavior in contrast to the saw-cut surfaces previously used; (3) the influence of time of deformation on saturated simulated gouges of clay minerals; (4) the mechanical behavior of ultrafine particles, as they appear important in understanding the properties of gouge; and (5) permeability and porosity changes of simulated gouges. All of these studies should provide additional information on the behavior of simulated gouges within the next few months.

The immediate question is what can such studies contribute to our knowledge of natural fault zones? First, it should be pointed out, that even with the present state of knowledge, the laboratory experiments serve an important function in stimulating ideas which can serve to guide the field studies. They can help to focus much of the investigations by providing such questions as (1) does most of the displacement appear to be heterogeneous as opposed to homogeneously distributed in the fault zone; (2) is there evidence of concentrating displacements at the gouge-country rock interface; (3) what is the distribution of ultrafine material and its implication with respect to permeability; (4) what is the fracture pattern within the fault zone; (5) what is the fault zone composition, particularly with respect to clays; (6) what is the nature of the interface between the gouge and country rock and the nature of the country rock? As pointed out previously, the reasons for attempting such studies are numerous, but it should be emphasized that these

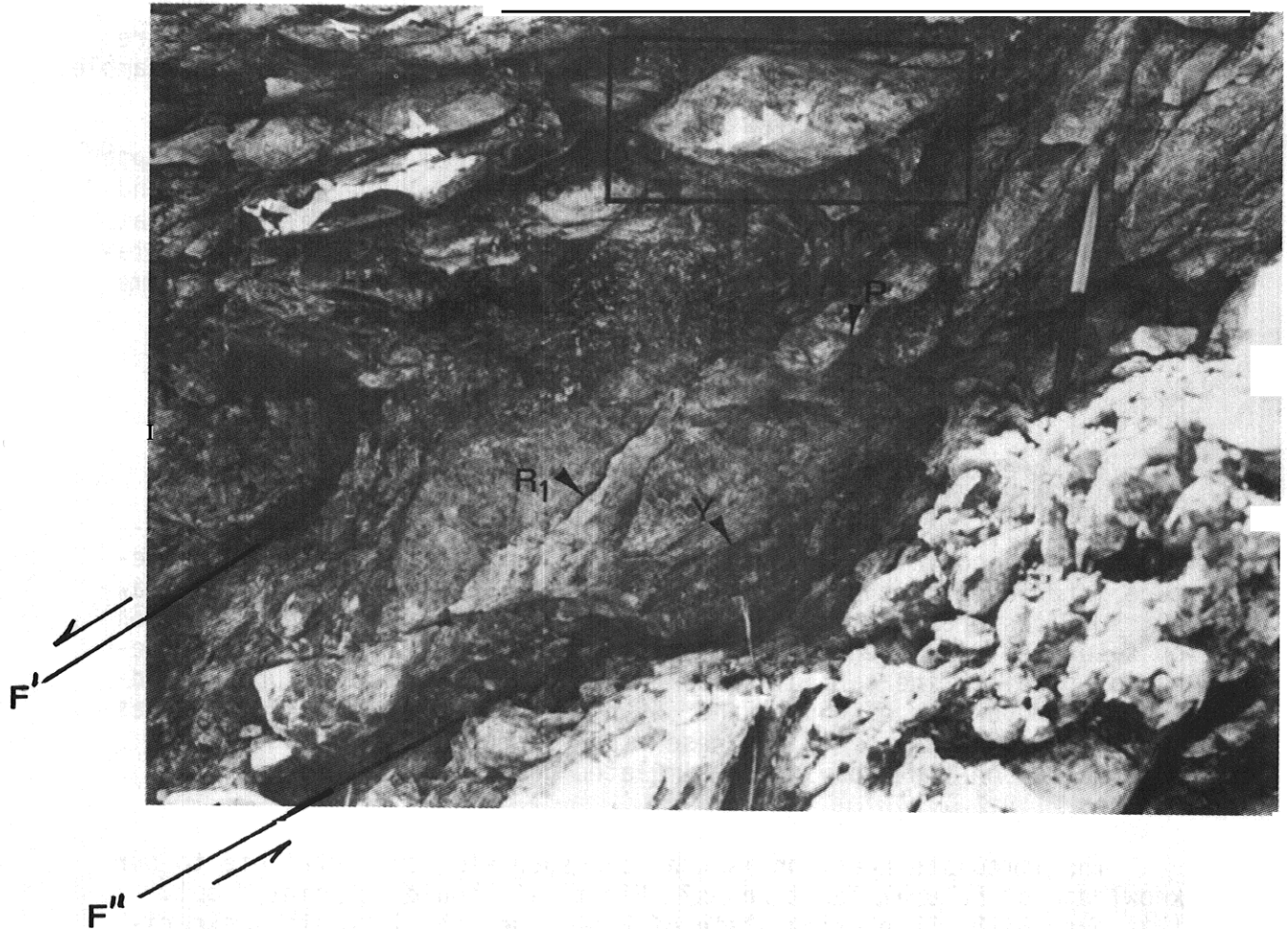


Figure 13. F' and F'' are the gouge zone boundaries. R1, P, and Y are the fractures shown. Pen used for scale is 12 cm long.

experiments were not designed as scale models of larger fault zones. They were envisioned as attempts to look at the processes in simulated fault zones of a few millimeters thick and a few centimeters of displacement. It was hoped that if the processes operating in the laboratory specimens could be understood that some aspects might prove to be scale independent and thus could be applied to larger natural fault zones, but there is no a priori reason why this should be so and must be established. A way to try to establish a level of confidence in the laboratory experiments is to compare some of the results with the field conditions. One of the most useful techniques is to consider the physical changes within the simulated gouges and attempt to establish natural counterparts, first on faults of small displacement or narrow gouge width and gradually extend this to larger fault zones. Specifically, one could try to extrapolate (1) the fabric and fracture pattern as recognized in simulated gouges to natural fault zones; (2) the concept that displacements are heterogeneous, primarily occurring at or close to the interface with the country rock or parallel to the gouge-country rock boundary; (3) the influence of the country rock-gouge interaction to recognize areas of seismic versus aseismic slip; and (4) to investigate variations in composition of natural fault gouges. If a reasonable correlation between such features in simulated gouge zones deformed in the laboratory and natural fault zones could be established, then additional information on the mechanical behavior of laboratory specimens might be used with more confidence.

To date, the field study of the fractures developed within the Motagua Fault and other fault zones have been very rewarding. Generally, the fracture pattern developed in simulated gouges in the laboratory is found to have counterparts in natural fault zones. The fractures R1, R2, P and X have all been recognized. These are all well developed. Not only has their presence been recognized, but their geometrical relations to each other and to the boundaries of the fault zone are very close to that found in the experimental studies. At the same time, some differences between the experimental results and the field relations have been observed. These differences are: (1) fracture type T has not been clearly identified from field observations; (2) the R2 in the field are less developed than in the experiment; (3) the Y fractures are dominant in the field and not in the experiment.

The obvious difference between the experimental studies and the field situation may be the larger amount of displacement along the natural faults studied. This may well suggest why the Y fractures are dominant in the field. This is corroborated to some extent by a few laboratory experiments which have been carried to relatively large displacements (Mendel et al., 1977). In these, the Y fractures increase in importance relative to the other fractures. These experiments and the field evidence, would suggest that as the displacement increases, secondary displacement zones or surfaces parallel to the fault zone boundaries may be established and the total displacement of the fault zone may be taken up in part or totally by movement along these secondary fractures. It is possible that the amount of displacement on any fracture varies along the strike of the fault zone and in time.

Another significant feature of the natural fault zones is that no other dominant fracture types have been identified in the field that have not been recognized in experimental studies. However, there are fractures in the naturally deformed rocks which do not fit any of the above types. This may be due to a random fracture pattern associated with the original emplacement of the serpentinite along the Motagua Fault, or due to rotated fractures of any of the above types. Additionally, no concrete evidence has been found substantiating the existence of extension fractures within the shear zones, i.e., all fractures recognized to be shear fractures. At this time the data are still preliminary so their existence should not be precluded.

CONCLUSIONS

Our experimental studies of simulated fault gouge and attempts to correlate some of the results to natural fault zones suggest the following conclusions.

1. When fracture and cataclasis are the principle mechanisms of gouge behavior the deformation of the gouge becomes heterogeneous with very small initial displacement. The major displacement occurs in a very narrow zone at or parallel to the gouge-rock interface.
2. When ductile flow is the principle mechanism of gouge behavior, the deformation is quite homogeneous, with the displacement taken up uniformly across the full width of the fault zone. The zone of displacement would be correspondingly wider than that expected within the cataclastic regime.
3. To date, within the field of fracture and cataclastic behavior of the simulated gouges, there are no diagnostic features separating stick-slip from stable sliding, that is gouges of different compositions showing either stick-slip or stable sliding develop similar fabrics.
4. However, corresponding with the change from cataclastic behavior to ductile flow in simulated gouges of calcite there is a change in sliding mode from stick-slip to stable sliding. It does appear that ductile flow is uniquely associated with stable sliding.
5. There is a predictable pattern of fractures developed within the simulated gouges, with the most pervasive fracture the Riedel shear.
6. Attempts to recognize these fractures produced in laboratory experiments with those developed at selected field locations, have shown a high degree of correlation. Further field studies to document other features appear warranted at this time.

REFERENCES

- Allen, C. R. and Smith, S. W., 1966, Pre-earthquake and post-earthquake surficial displacements in Parkfield earthquakes of June 27-29, 1966, Monterey and San Luis Obispo Counties, California, preliminary report: *Seismol. Soc. Amer. Bull.*, v. 56, p. 966-967.
- Brown, R. D., Jr. and Vedder, J. G., 1967, Surface tectonic fractures along the San Andreas fault: in *The Parkfield-Chalome, California, earthquakes of June-August, 1966*: U.S. Geol. Survey Prof. Paper 579, p. 11-23.
- Byerlee, J., Mjachkin, V., Summers, R., and Voevoda, O., 1978, Structures developed in fault gouge during stable sliding and stick-slip: *Tectonophysics*, v. 44, p. 161-171.
- Byerlee, J. D. and Summers, R., 1973, The effect of fault gouge on the stability of sliding on saw-cuts in granite (Abstract): *EOS, Trans. AGU*, v. 54, p. 1210.
- Byerlee, J. D. and Summers, R., 1976, A note on the effect of fault gouge thickness of fault stability: *Int. J. Rock Mech. Min. Sci. & Geomech. Abstr.*, v. 13, p. 35-36.
- Cloos, H., 1928, Experimente zur inneren Tektonik: *Centralbl. Mineral. Geol. w. Pal.*, v. 1928B, p. 609-621.
- Cloos, E., 1932, "Feather" joints as indicators of the direction of movement on faults, thrusts, joints, and magmatic contacts: *Natl. Acad. Sci. Proc.*, v. 18, p. 387-395.
- Conrad, R. E., II and Friedman, M., 1976, Microscopic feather fractures in the faulting process: *Tectonophysics*, v. 33, p. 187-198.
- Dunnet, D., 1969, A technique of finite strain analysis using elliptical particles: *Tectonophysics*, v. 7, p. 117-136.
- Engelder, J. T., 1973, Quartz fault-gouge: Its generation and effect on the frictional properties of sandstone: *Ph.D. Dissertation*, Dept. of Geology, Texas A&M University, August, 1973, 154 p.
- Engelder, J. T., 1974, Cataclasis and the generation of fault gouge: *Geol. Soc. Amer. Bull.*, v. 85, p. 1515-1522.
- Engelder, J. T., Logan, J. M., and Handin, J., 1975, The sliding characteristics of sandstone on quartz fault-gouge: *Pageoph*, v. 113, p. 69-86.
- Etheridge, M. A. and Wilkie, J. C., 1979, The geometry and microstructure of a range of QP-mylonite zones--a field test of the recrystallized grain size palaeopiezometer: *U.S.G.S. Conference on Fault Zone Properties* (this volume), Palm Springs, CA.

- Freund, Raphael, 1974, Kinematics of transform and transcurrent faults: *Tectonophysics*, v. 21, p. 93-134.
- Griggs, D. T., Turner, F. J., and Heard, H. C., 1960, Deformation of rocks at 500° to 800°C: *Geol. Soc. Am. Memoir* 79, p. 39-104.
- Higgins, M. W., 1971, Cataclastic rocks: *U.S.G.S. Prof. Paper* 687, 97 p.
- Higgs, N. G. and Logan, J. M., 1977, Effects of temperature on gouge deformation in sliding friction experiments (Abstract): *EOS Trans. Am. Geophys. Union*, v. 58, p. 1228.
- Jackson, R. E. and Dunn, D. E., 1974, Experimental sliding friction and cataclasis of foliated rocks: *Int. J. Rock Mech. Min. Sci. and Geomech. Abstr.*, v. 11, p. 235-249.
- Jaeger, J. C. and Gay, N. C., 1974, Behavior of lightly confined granular material: *Int. J. Rock Mech. Min. Sci. and Geomech. Abstr.*, v. 11, p. 295-301.
- Lajtai, E. Z., 1969, Mechanics of second order faults and tension gashes: *Geol. Soc. America Bull.*, v. 80, p. 2253-2272.
- Logan, J. M., 1975, Friction in rocks: *Revs. Geophys. Space Phys.*, v. 13, n. 3, p. 358-361.
- Logan, J. M. and Shimamoto, T., 1976, The influence of calcite gouge on frictional sliding of Tennessee sandstone (Abstract): *EOS, Trans. American Geophys. Union*, v. 57, p. 1011.
- Mandl, G., de Jong, L. N. J., and Maltha, A., 1977, Shear zones in granular materials--An experimental study of their structure and mechanical genesis: *Rock Mech.*, v. 9, p. 95-144.
- McKinstry, M. E., 1953, Shears of second order: *Am. Jour. Sci.*, v. 251, p. 401.
- Morgenstern, N. R. and Tchalenko, J. S., 1967, Microscopic structures in kaolin subjected to direct shear: *Geotechnique*, v. 17, p. 309-328.
- Oertel, G., 1965, The mechanism of faulting in clay experiments: *Tectonophysics*, v. 2, p. 343-393.
- Raleigh, C. B., Healy, J. H., and Bredehoaft, J. D., 1972, Faulting and crustal stress at Rangely, Colorado: in *Flow and Fracture of Rocks, The Griggs Volume*, H. C. Heard, I. Y. Borg, N. L. Carter, C. B. Raleigh, eds., *Am. Geophys. Union, Geophys. Mono.* 16, p. 275-284.
- Ramsay, J. G., 1967, *Folding and fracturing of rocks*: McGraw-Hill, New York, 568 p.

- Riedel, W., 1929, Zur mechanik geologischer Brucherscheinungen: Centralbl. Mineral. Geol. u. Pal., v. 19298, p. 354-368.
- Boering, C., 1968, The geometrical significance of natural en echelon crack arrays: Tectonophysics, v. 5, p. 107-123.
- Shimamoto, T., 1977, Effects of fault-gouge on the frictional properties of rocks: An Experimental study: Ph.D. Dissertation, Dept. of Geology, Texas A&M Univ., Dec. 1977, 198 p.
- Stuart, W. D., 1974, Diffusionless dilatancy model for earthquake precursors: Geophys. Res. Letters, v. 1, p. 261-264.
- Summers, R. and Byerlee, J. D., 1974, The effect of hydration on the frictional properties of fault gouge (Abstract): EOS, Trans. AGU, v. 56, p. 1194.
- Summers, R. and Byerlee, J. D., 1977, A note on the effect of fault gouge composition on the stability of frictional sliding: Int. J. Rock Mech. Min. Sci. & Geomech. Abstr., v. 14, p. 155-160.
- Summers, R., Mjachkin, V., Voevoda, O., and Byerlee, J. D., 1976, Shear zones developed in fault gouge during stable sliding and stick-slip (Abstract): EOS, Trans. AGU, v. 57, p. 1011.
- Tchalenko, J. S., 1970, Similarities between shear zones of different magnitude: Geol. Soc. Amer. Bull., v. 81, p. 1625-1640.
- Tchalenko, J. S., 1973, Surface fracture patterns along the San Andreas Fault: in Proc. Conf. Tectonic Problems of the San Andreas Fault System, R. L. Kovach and Amos Nur eds., Stanford Univ. Pubs., Geol. Sci., v. 13, p. 248-250.
- Wallace, R. E. and Roth, E. F., 1967, Rates and patterns of progressive deformation: in Parkfield-Chalome, California, earthquakes of June-August, 1966: U.S. Geol. Sur. Prof. Paper 579, p. 23-40.